

Supporting Information

Cyclodextrin Dimer as Supramolecular Reaction Platform for Aqueous Organometallic Catalysis.

Claire Blaszkiewicz,^{ab} Hervé Bricout,^a Estelle Léonard,^c Christophe Len,^c David Landy,^d Christine Cézard,^b Florence Djedaïni-Pilard,^b Eric Monflier^a and Sébastien Tilloy^{*a}

^a *Unité de Catalyse et de Chimie du Solide (UCCS), CNRS, UMR 8181, Université d'Artois, Rue Jean Souvraz, SP 18, F-62307 Lens, France. Fax: + 33321791755; Tel: 33321791754; E-mail: sebastien.tilloy@univ-artois.fr*

^b *Laboratoire des Glucides, CNRS FRE 3517, Université de Picardie Jules Verne, 80039 Amiens, France*

^c *Transformations Intégrées de la Matière Renouvelable - EA 4297 UTC/ESCOM, Centre de Recherches de Royallieu, BP 20529, rue Personne de Roberval, F-60205 Compiègne cedex, France*

^d *Unité de Chimie Environnementale et Interactions sur le Vivant (UCEIV) – EA 4492, Université du Littoral Côte d'Opale 145, Avenue Maurice Schumann, MREI 1, F-59140 Dunkerque, France*

<u>Experimental part</u>	S3
I.1) Materials and apparatus.....	S3
I.2) <i>N,N'</i> -bis[(6 ^A -deoxy-β-cyclodextrin)yl]biphenyl-4,4'-dicarboxamide (CD-dim) synthesis.	S3
I.3) [Rh(COD)(Phosphane) ₂ ⁺ , BF ₄ ⁻] complexes syntheses.....	S5
I.4) Determination of stoichiometry and association constant of the inclusion complexes.....	S5
I.5) Hydroformylation tests.....	S6
I) <u>Compounds NMR characteristics</u>	S7
II.1) Disuccinimidyl biphenyl-4,4'-dicarboxylate.....	S7
II.2) <i>N,N'</i> -bis[(6 ^A -deoxy-β-cyclodextrin)yl]biphenyl-4,4'-dicarboxamide (CD-dim).....	S7
II.3) [Rh(COD)(1) ₂ ⁺ , BF ₄ ⁻] complex.....	S7
II.4) [Rh(COD)(TPPTS) ₂ ⁺ , BF ₄ ⁻] complex.....	S7
II) <u>Compounds NMR spectra (and Maldi spectrum of CD-dim)</u>	S8
III.1) Disuccinimidyl biphenyl-4,4'-dicarboxylate.....	S8
III.2) <i>N,N'</i> -bis[(6 ^A -deoxy-β-cyclodextrin)yl]biphenyl-4,4'-dicarboxamide (CD-dim).....	S10
III.3) [Rh(COD)(1) ₂ ⁺ , BF ₄ ⁻] complex.....	S16
III.4) [Rh(COD)(TPPTS) ₂ ⁺ , BF ₄ ⁻] complex.....	S22
III) <u>1D NMR studies of the interactions between the different compounds</u>	S25
IV.1) Evidences of interaction between Phosphane 1 and β-CD.....	S25
IV.2) Evidences of interaction between Phosphane 1 and CD-dim	S26
IV.3) Evidences of interaction between [Rh(COD)(1) ₂ ⁺ , BF ₄ ⁻] complex and β-CD.....	S27
IV.4) Evidences of interaction between [Rh(COD)(1) ₂ ⁺ , BF ₄ ⁻] complex and CD-dim	S29
IV.5) Evidences of non-interaction between [Rh(COD)(TPPTS) ₂ ⁺ , BF ₄ ⁻] complex and β-CD or CD-dim	S31
IV) <u>Inclusion complexes stoichiometry and association constants</u>	S34
V.1) Interaction between Phosphane 1 and β-CD.....	S34
V.2) Interaction between Phosphane 1 and CD-dim	S36
V.3) Interaction between [Rh(COD)(1) ₂ ⁺ , BF ₄ ⁻] complex and β-CD.....	S37
V.4) Interaction between [Rh(COD)(1) ₂ ⁺ , BF ₄ ⁻] complex and CD-dim	S37
V) <u>T-ROESY studies of the inclusion complexes</u>	S38
VI.1) T-ROESY of a Phosphane 1 and β-CD mixture.....	S38
VI.2) T-ROESY of a Phosphane 1 and CD-dim mixture.....	S39
VI.3) T-ROESY of a [Rh(COD)(1) ₂ ⁺ , BF ₄ ⁻] complex and β-CD mixture.....	S40
VI.4) T-ROESY of a [Rh(COD)(1) ₂ ⁺ , BF ₄ ⁻] complex and CD-dim mixture.....	S41
VI) <u>Molecular dynamics simulations</u>	S42

VII) <u>Tensiometry study of an aqueous solution of CD-dim</u>	S46
VIII) <u>Catalysis results</u>	S46

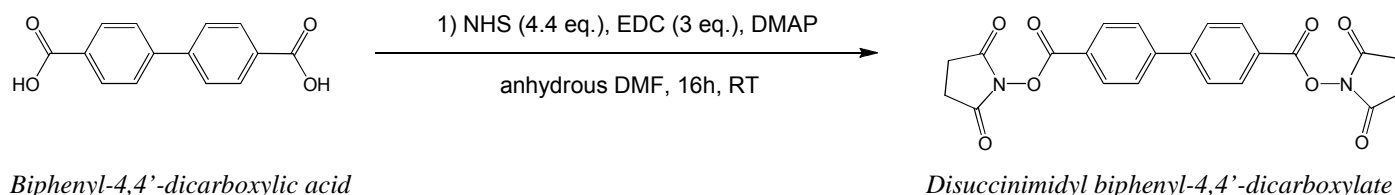
I) Experimental part

I.1) Materials and apparatus

All chemicals were purchased from Fisher Scientific and Aldrich Chemicals in their highest purity. All solvents were used as supplied without further purification. Distilled water was used in all experiments. NMR spectra were recorded on a Bruker DRX300 spectrometer (300 MHz for ^1H nuclei), or on a Bruker DRX500 spectrometer (500 MHz for ^1H nuclei), or on a Bruker IPSO600 spectrometer (600 MHz for ^1H nuclei). DMSO- D_6 (99.80% isotopic purity) and D_2O (99.92% isotopic purity) were purchased from Euriso-Top. The correct assignments of the chemical shifts were confirmed by two-dimensional correlation measurements attained by ^1H - ^1H COSY, ^1H - ^{13}C HSQC and ^1H - ^{13}C HMBC experiments. Mass spectra were recorded on a MALDI-TOF/TOF Bruker Daltonics Ultraflex II in positive reflectron mode with 2,5-DHB as matrix.

I.2) *N,N'*-bis[(6^A-deoxy- β -cyclodextrin)yl]biphenyl-4,4'-dicarboxamide (CD-dim) synthesis

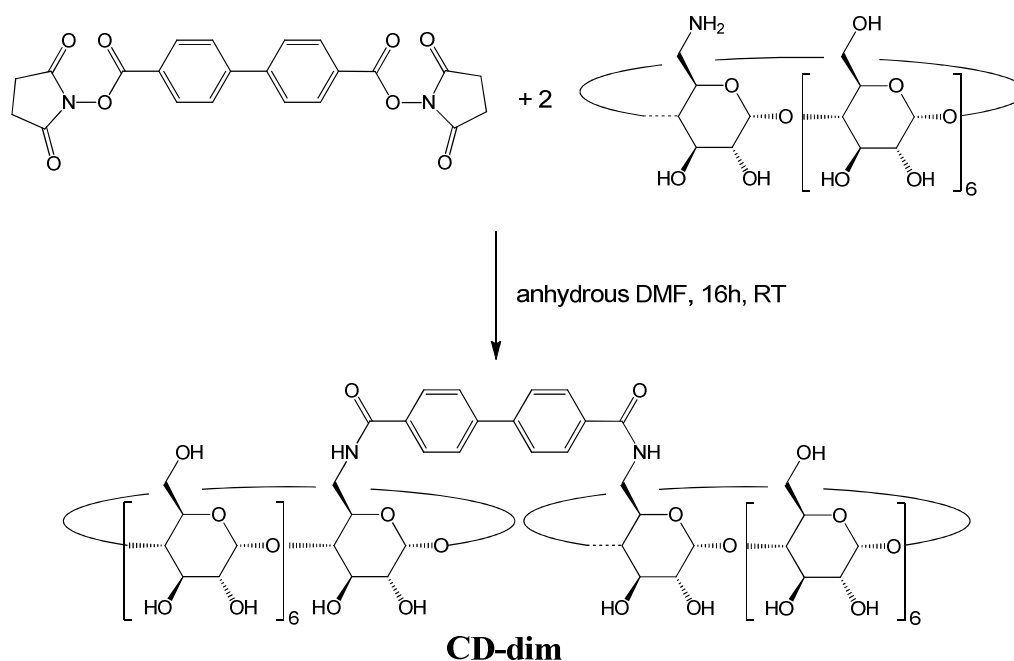
I.2.1) First step : Synthesis of Disuccinimidyl biphenyl-4,4'-dicarboxylate :



Scheme S1: Disuccinimidyl biphenyl-4,4'-dicarboxylate synthesis

To a solution of biphenyl-4,4'-dicarboxylic acid (1 g, 4.13 mmol) in anhydrous *N,N*-dimethylformamide (20 mL) were added at room temperature and under N_2 , *N*-hydroxysuccinimide (NHS, 2.09 g, 18.16 mmol), *N*-(3-dimethylaminopropyl)-*N'*-ethylcarbodiimide hydrochloride (EDC, 2.37 g, 12.38 mmol) and 4-(dimethylamino)pyridine (DMAP, 0.10 g, 0.83 mmol). The reaction mixture was stirred at room temperature under N_2 overnight. After reaction, the solvent was removed under reduced pressure. The residue was then dissolved in dichloromethane (200 mL) and this solution was washed with water (200 mL), dried with anhydrous K_2SO_4 and evaporated to dryness under vacuum. The residue was dissolved in 10 mL of anhydrous *N,N*-dimethylformamide and recrystallized at 0°C to give disuccinimidyl biphenyl-4,4'-dicarboxylate as a white product (1.44 g, yield = 82%).

I.2.2) Second step : Coupling of disuccinimidyl biphenyl-4,4'-dicarboxylate with 6^A-deoxy-6^A-amino-β-cyclodextrin

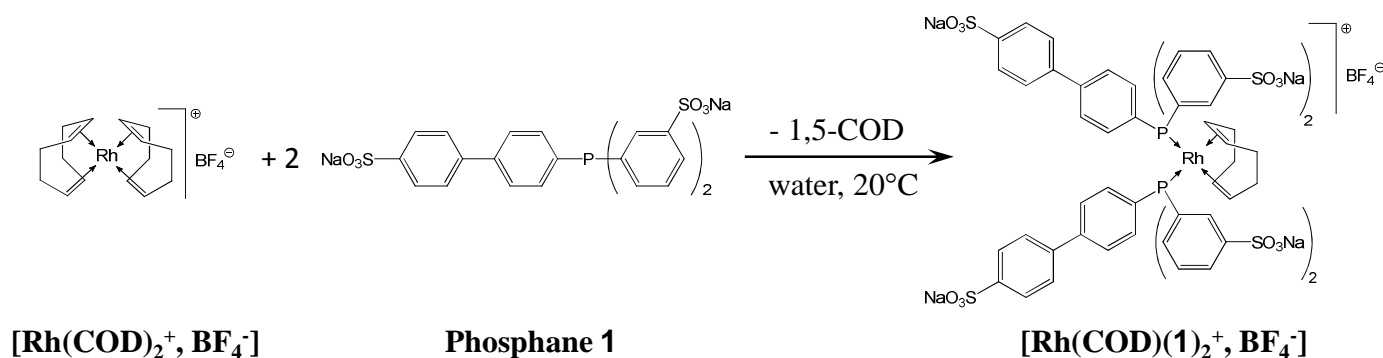


Scheme S2: CD-Dim synthesis from 6^A-deoxy-6^A-amino-β-cyclodextrin

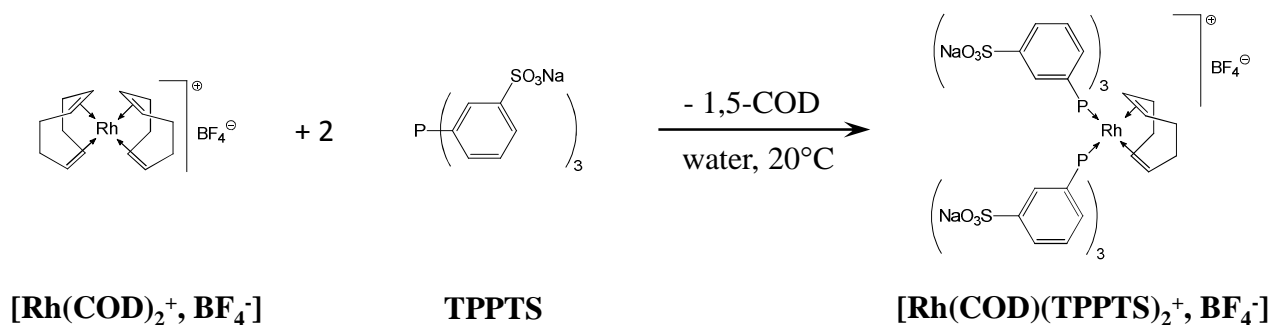
Disuccinimidyl biphenyl-4,4'-dicarboxylate (500mg, 1.15 mmol) and 6^A-deoxy-6^A-amino-β-cyclodextrin (2.2 eq) were dissolved in 20 mL of anhydrous *N,N*-dimethylformamide under N₂ and stirred at room temperature. After a day, the reaction mixture was poured into acetone (1 L) to precipitate the CD compounds. The precipitate was collected and washed with acetone and then dried under vacuum. The crude product was dialyzed for 24 h on a 100-500 MW dialysis membrane. Purification by reversed-phase chromatography (eluted with water/methanol 90/10 to 10/90, flow: 20 mL.min⁻¹) afforded a white powder (1.58 g, yield = 55%).

I.3) [Rh(COD)(Phosphane)₂⁺, BF₄⁻] complexes syntheses

The [Rh(COD)(Phosphane)₂⁺, BF₄⁻] complexes were obtained quantitatively by stirring at room temperature [Rh(COD)₂⁺, BF₄⁻] with 2 equivalents of phosphane in water for 10 min. The formed 1,5-dicyclooctadiene was then removed by degasing the obtained solution.



Scheme S3: [Rh(COD)(1)₂⁺, BF₄⁻] synthesis from [Rh(COD)₂⁺, BF₄⁻]



Scheme S4: [Rh(COD)(TPPTS)₂⁺, BF₄⁻] synthesis from [Rh(COD)₂⁺, BF₄⁻]

I.4) Determination of stoichiometry and association constant of the inclusion complexes

Stoichiometries and association constants of the “phosphane / CD derivative” combinations were determined by isothermal titration calorimetry. Stoichiometries were also checked by NMR (Job plot). Stoichiometries of the “phosphane / Rhodium species” combinations were determined under nitrogen by NMR.

An isothermal calorimeter (ITC₂₀₀, MicroCal Inc., USA) was employed for determining the formation constant of the “phosphane / CD derivative” complexes. The titration protocol was used at 298 K with a 204.5 μL cell and a 40 μL syringe. Degassed aqueous solutions (phosphate buffer, pH=6.5) were employed for all experiments. In the case of TPPTS complexes, a 0.5mM cyclodextrin solution (β -CD or **CD-dim**) was titrated by a 5mM TPPTS solution. In the case of phosphane **1** complexes, a 0.05mM phosphane **1** solution was titrated by a 0.5mM cyclodextrin solution (β -CD or **CD-dim**). After the addition of an initial aliquot of 0.4 μL , 10 aliquots of 3.7 μL of the syringe solution were delivered (over 7.4 s for each injection). The corresponding heat flow was recorded as a function of time. The time interval between two consecutive injections was 150 s and agitation speed was 1000 rpm for all experiments. In addition, the heat consecutive to dilution was eliminated by performing blank titrations. The areas under the peak following each injection (obtained by integration of the raw signal) were then expressed as the heat effect per mole of added phosphane or cyclodextrin. Each titration experiment was performed three times to assess reproducibility of the results. Binding constants and inclusion enthalpies were finally determined by nonlinear regression analysis of the binding isotherms using a built-in binding model (one set of sites) within MicroCal Origin 7.0 software package (MicroCal, Northampton, MA). The n number of available sites per cyclodextrin molecule was taken into account during the regression analysis.

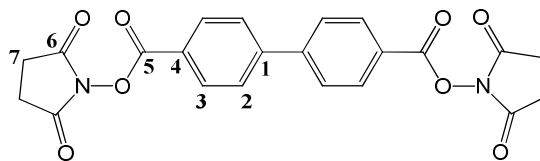
I.5) Hydroformylation tests

All hydroformylation reactions were performed under nitrogen using standard Schlenk techniques. In a typical experiment, Rh(acac)(CO)₂ (5.5 mg; 21 μmol), phosphane (105 μmol ; 5 eq.) and CD derivative (210 μmol of CD cavity; 10 eq.) were dissolved in 6 mL of water. The resulting aqueous phase and the olefin (10.5 mmol; 500 eq.) were charged under nitrogen into a 25 mL reactor heated at the desired temperature. The mixture was mechanically stirred using a multipaddle unit (1500 rpm) and the autoclave was pressurized under 50 atm CO/H₂ (1:1). Once the reaction was complete, the organic phase was analyzed by ¹H-NMR and by gas chromatography on a Shimadzu GC-17A gas chromatograph equipped with a polydimethylsiloxane capillary column (30 m x 0.32 mm) and a flame ionization detector (GC:FID).

II) Compounds NMR characteristics

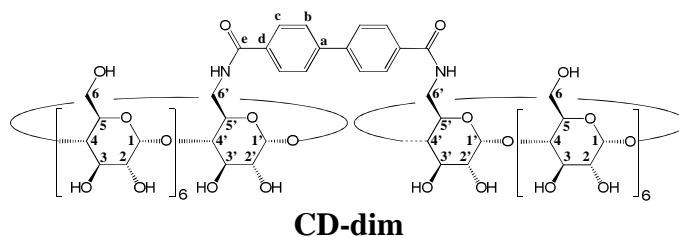
II.1) Disuccinimidyl biphenyl-4,4'-dicarboxylate

^1H NMR (300 MHz, $\text{DMSO-}d_6$): $\delta(\text{ppm}) = 2.92$ (s, 8H, H-7), 8.08 (d, $^3J_{\text{H,H}} = 8.5$ Hz, 4H, H-2), 8.24 (d, $^3J_{\text{H,H}} = 8.5$ Hz, 4H, H-3). $^{13}\text{C}\{^1\text{H}\}$ NMR (75.5 MHz, $\text{DMSO-}d_6$): $\delta(\text{ppm}) = 25.59$ (s, C-7), 124.45 (s, C-1), 128.32 (s, C-2), 130.84 (s, C-3), 144.81 (s, C-4), 161.54 (s, C-5), 170.34 (s, C-6).



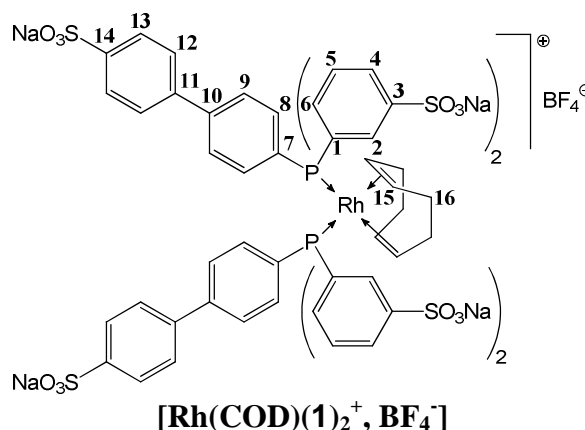
II.2) N,N' -bis[(6^A-deoxy- β -cyclodextrin)yl] biphenyl-4,4'-dicarboxamide (CD-dim)

^1H NMR (600 MHz, D_2O): $\delta(\text{ppm}) = 3.10$ -4.18 (m, 84H, H-2, H-2', H-3, H-3', H-4, H-4', H-5, H-5', H-6, H-6'), 4.85-5.13 (m, 14H, H-1, H-1'), 7.70 (d, $^3J_{\text{H,H}} = 8.2$ Hz, 4H, H-b), 7.78 (d, $^3J_{\text{H,H}} = 8.2$ Hz, 4H, H-c). $^{13}\text{C}\{^1\text{H}\}$ NMR (150 MHz, D_2O): $\delta(\text{ppm}) = 41.09$ (s, C-6'), 59.20-60.50 (m, C-6), 70.25-73.25 (m, C-2, C-2', C-3, C-3', C-5, C-5'), 80.20-83.80 (m, C-4, C-4'), 101.20-102.25 (m, C-1, C-1'), 127.20 (s, C-b), 127.73 (s, C-c), 132.48 (s, C-a), 142.81 (s, C-d), 169.27 (s, C-e).



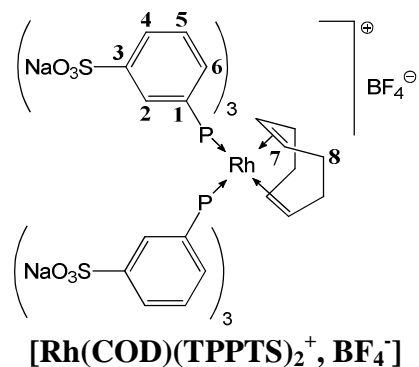
II.3) $[\text{Rh}(\text{COD})(1)_2]^+, \text{BF}_4^-$ complex

^1H NMR (300 MHz, D_2O): $\delta(\text{ppm}) = 2.31$ (broad d, $^2J_{\text{H,H}} = 8$ Hz, 4H, H-16), 2.61 (broad d, $^2J_{\text{H,H}} = 8$ Hz, 4H, H-16'), 4.75 (broad s, 4H, H-15), 7.23 (broad t, $^3J_{\text{H,H}} = ^3J_{\text{H,P}} = 7.6$ Hz, 4H, H-8), 7.39 (d, $^3J_{\text{H,H}} = 7.6$ Hz, 4H, H-9), 7.51 (t, $^3J_{\text{H,H}} = 7.7$ Hz, 4H, H-5), 7.65 (m, 8H, H-6 and H-12), 7.82 (d, $^3J_{\text{H,H}} = 7.9$ Hz, 4H, H-13), 7.92 (d, $^3J_{\text{H,H}} = 7.7$ Hz, 4H, H-4), 8.41 (broad s, 4H, H-2). $^{13}\text{C}\{^1\text{H}\}$ NMR (75.5 MHz, D_2O): $\delta(\text{ppm}) = 33.04$ (s, C-16), 104.20 (s, C-15), 129.00 (s, C-13), 130.00 (s, C-9), 130.52 (s, C-12), 131.41 (s, C-4), 132.66 (s, C-5), 134.93 (s, C-2), 136.78 (s, C-8), 139.81 (s, C-6), 144-148 (C-1, C-3, C-7, C-10, C-11, C-14). $^{31}\text{P}\{^1\text{H}\}$ NMR (121.5 MHz, D_2O): $\delta(\text{ppm}) = 24.98$ (d, $^1J_{\text{P,Rh}} = 147.7$ Hz).



II.4) $[\text{Rh}(\text{COD})(\text{TPPTS})_2]^+, \text{BF}_4^-$ complex

^1H NMR (300 MHz, D_2O): $\delta(\text{ppm}) = 2.28$ (broad s, 4H, H-8), 2.58 (broad s, 4H, H-8'), 4.69 (broad s, 4H, H-7), 7.41 (broad s, 12H, H-5 and H-6), 7.86 (broad m, 6H, H-4), 8.04 (broad s, 6H, H-2). $^{13}\text{C}\{^1\text{H}\}$ NMR (75.5 MHz, D_2O): $\delta(\text{ppm}) = 32.96$ (s, C-8), 105.04 (s, C-7), 131.54 (s, C-4), 132.78 (s, C-5), 133.64 (s, C-2), 139.49 (s, C-6), 146.20 (s, C-1 / C-3). $^{31}\text{P}\{^1\text{H}\}$ NMR (121.5 MHz, D_2O): $\delta(\text{ppm}) = 26.56$ (d, $^1J_{\text{P,Rh}} = 148.4$ Hz).



III) Compounds NMR spectra

III.1) Disuccinimidyl biphenyl-4,4'-dicarboxylate

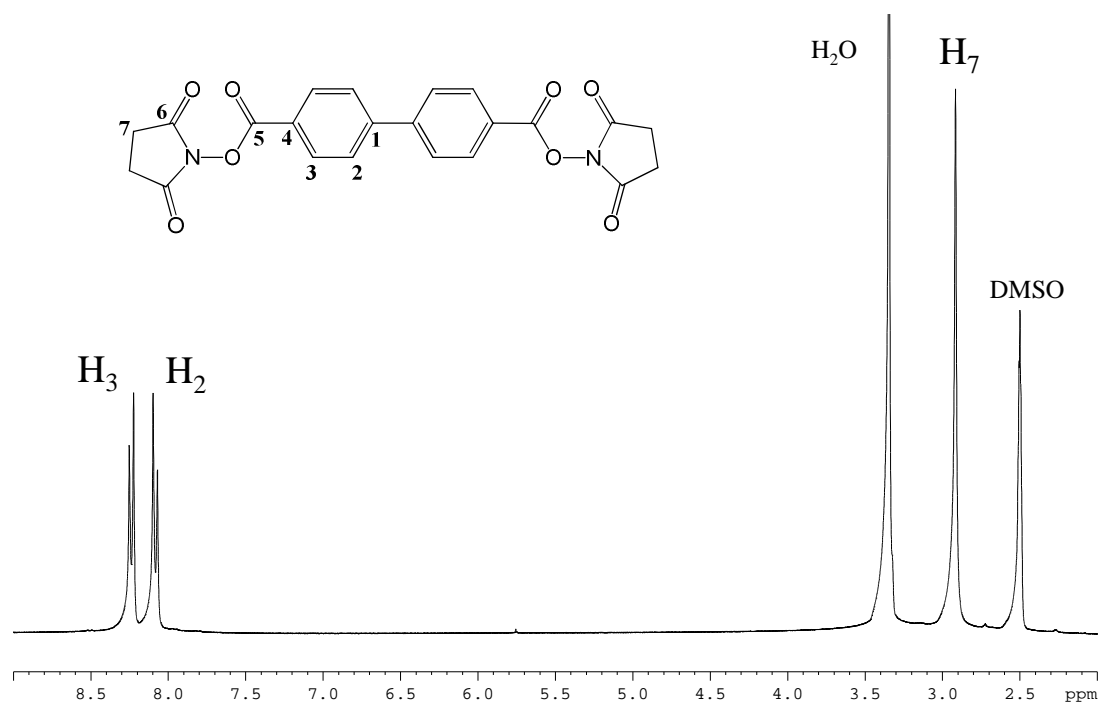


Figure S1: ^1H NMR spectrum of Disuccinimidyl biphenyl-4,4'-dicarboxylate (300 MHz, DMSO- D_6).

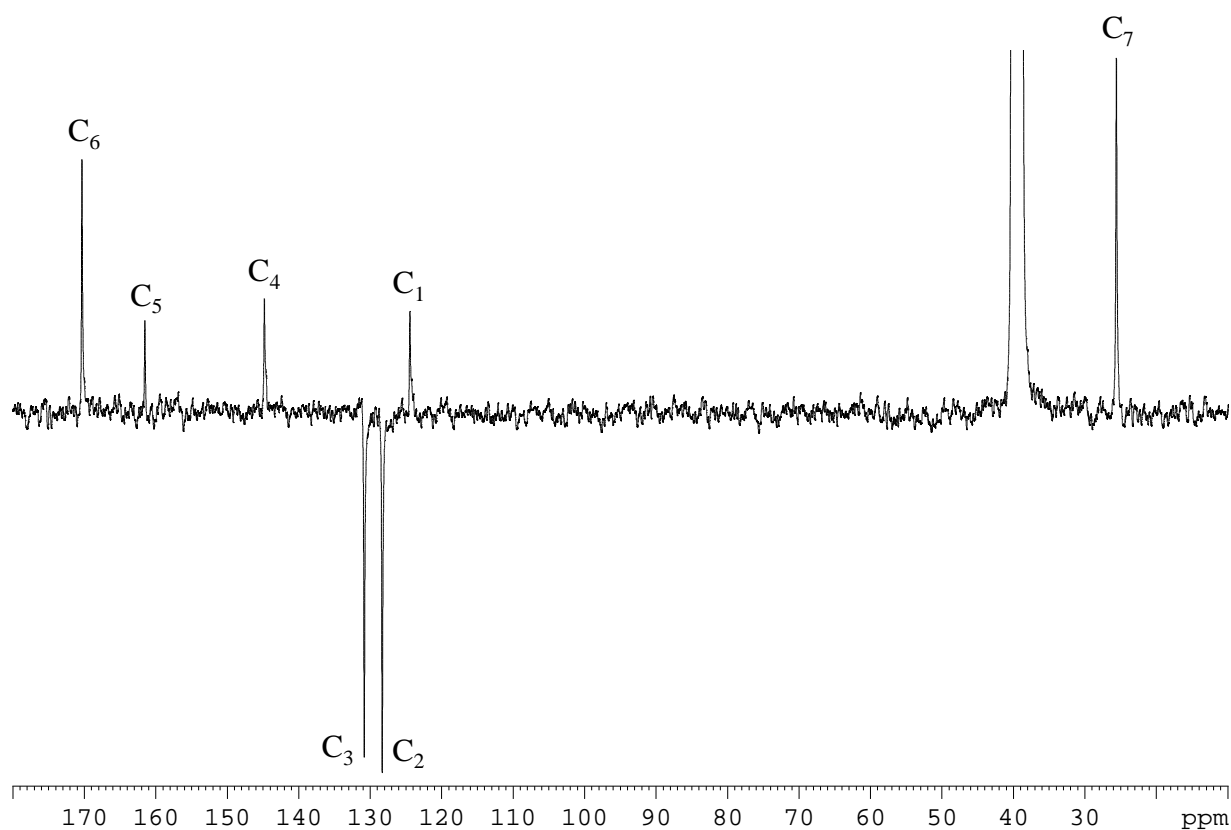


Figure S2: JMOD- ^{13}C NMR spectrum of Disuccinimidyl biphenyl-4,4'-dicarboxylate (75.5 MHz, DMSO- D_6).

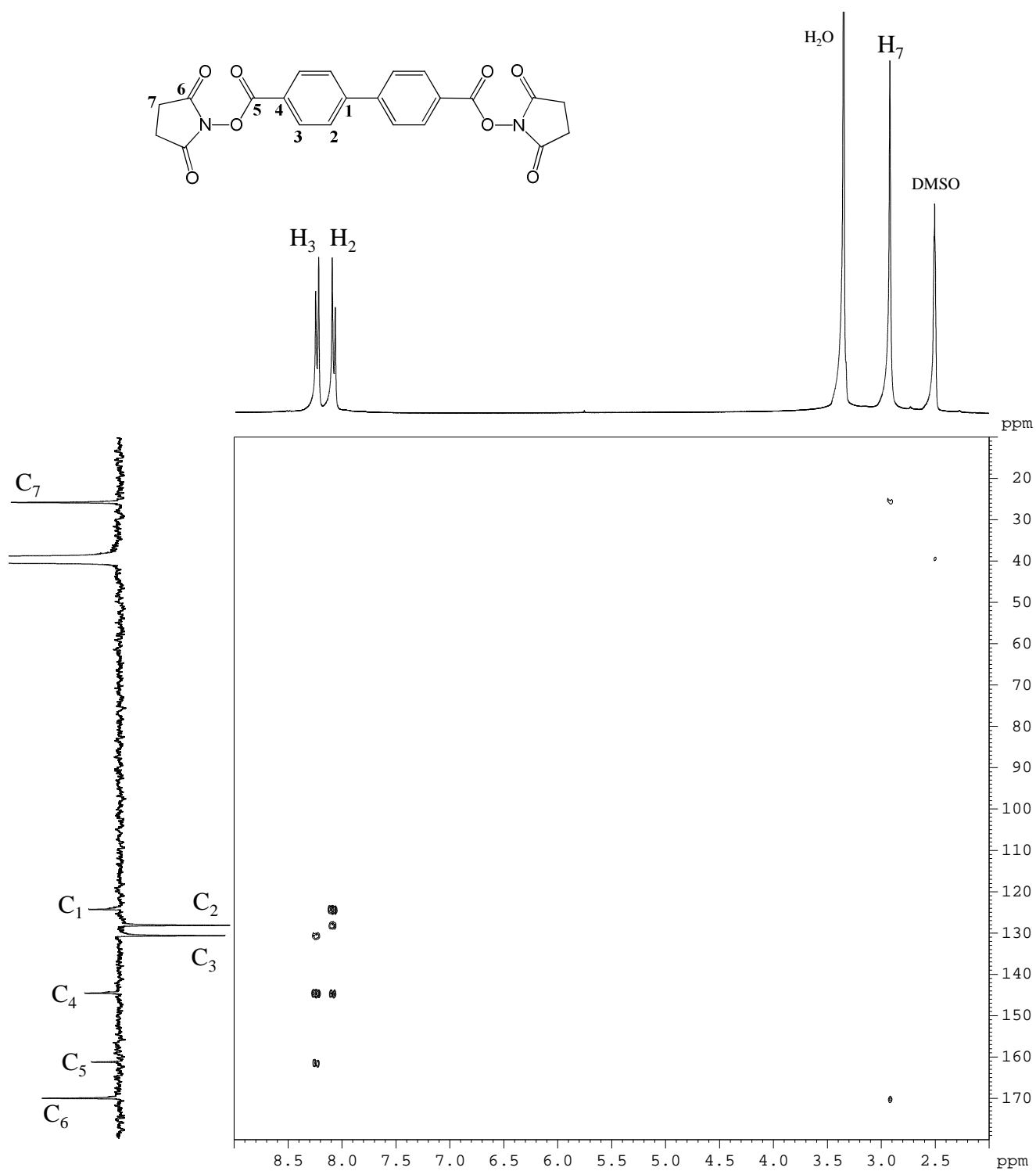


Figure S3: HMBC NMR spectrum of Disuccinimidyl biphenyl-4,4'-dicarboxylate (DMSO-D₆).

III.2) *N,N'*-bis[(6^A-deoxy-β-cyclodextrin)yl]biphenyl-4,4'-dicarboxamide (CD-dim)

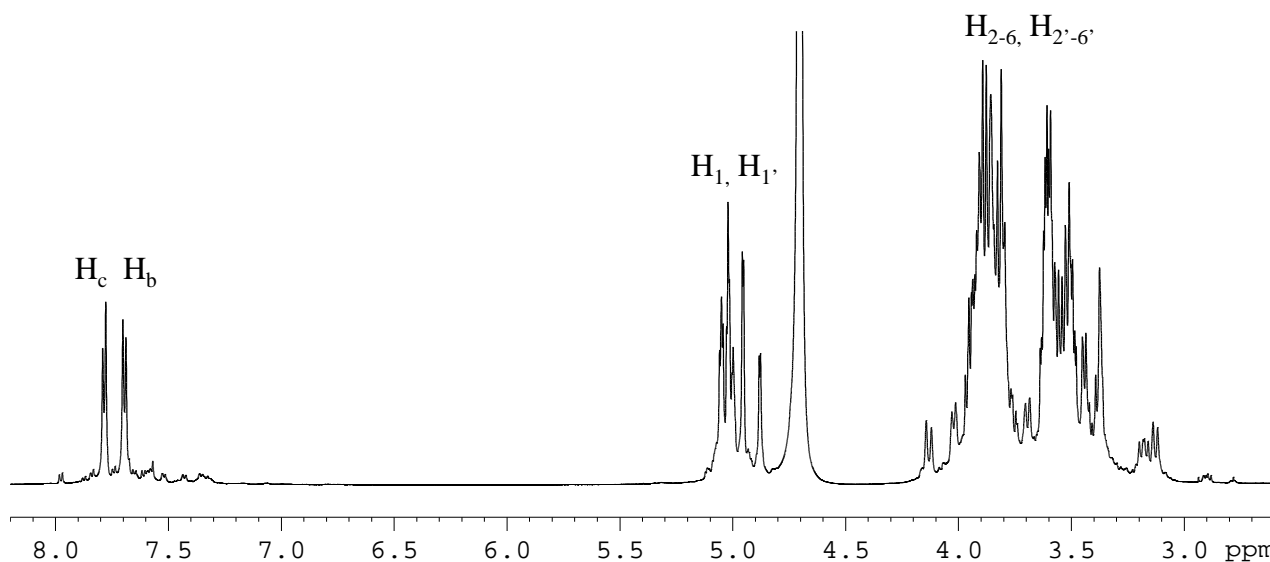
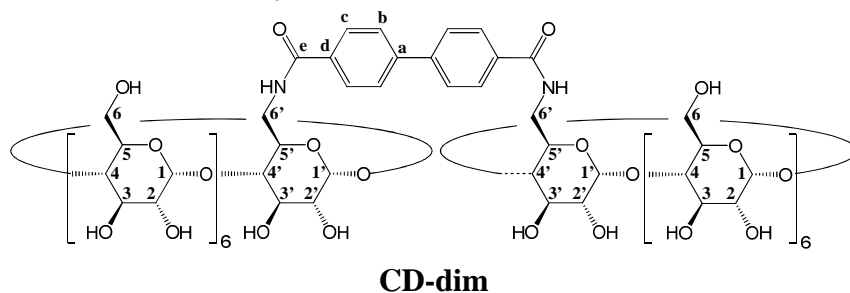


Figure S4: ¹H NMR spectrum of *N,N'*-bis[(6^A-deoxy-β-cyclodextrin)yl] biphenyl-4,4'-dicarboxamide (**CD-dim**) (600 MHz, D₂O).

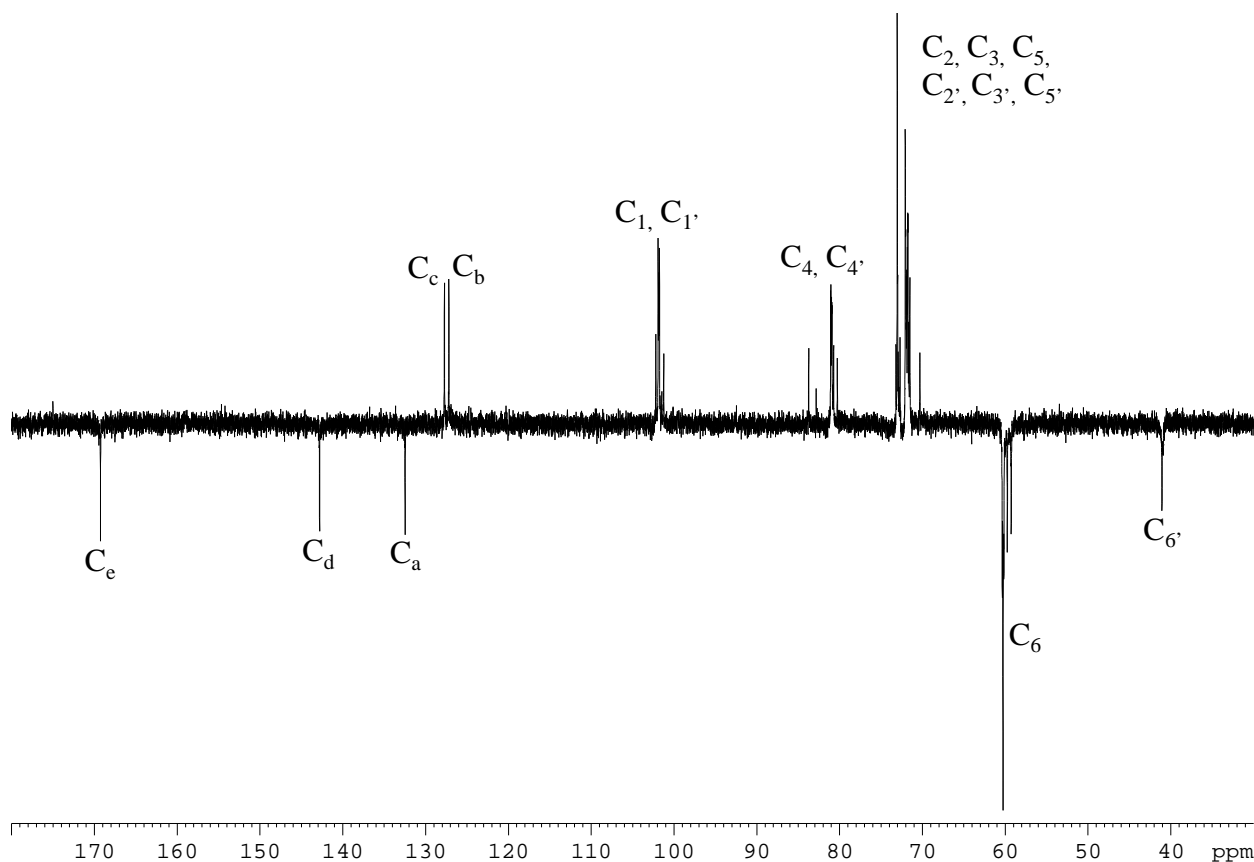


Figure S5: JMOD-¹³C NMR spectrum of *N,N'*-bis[(6^A-deoxy-β-cyclodextrin)yl] biphenyl-4,4'-dicarboxamide (**CD-dim**) (150 MHz, D₂O).

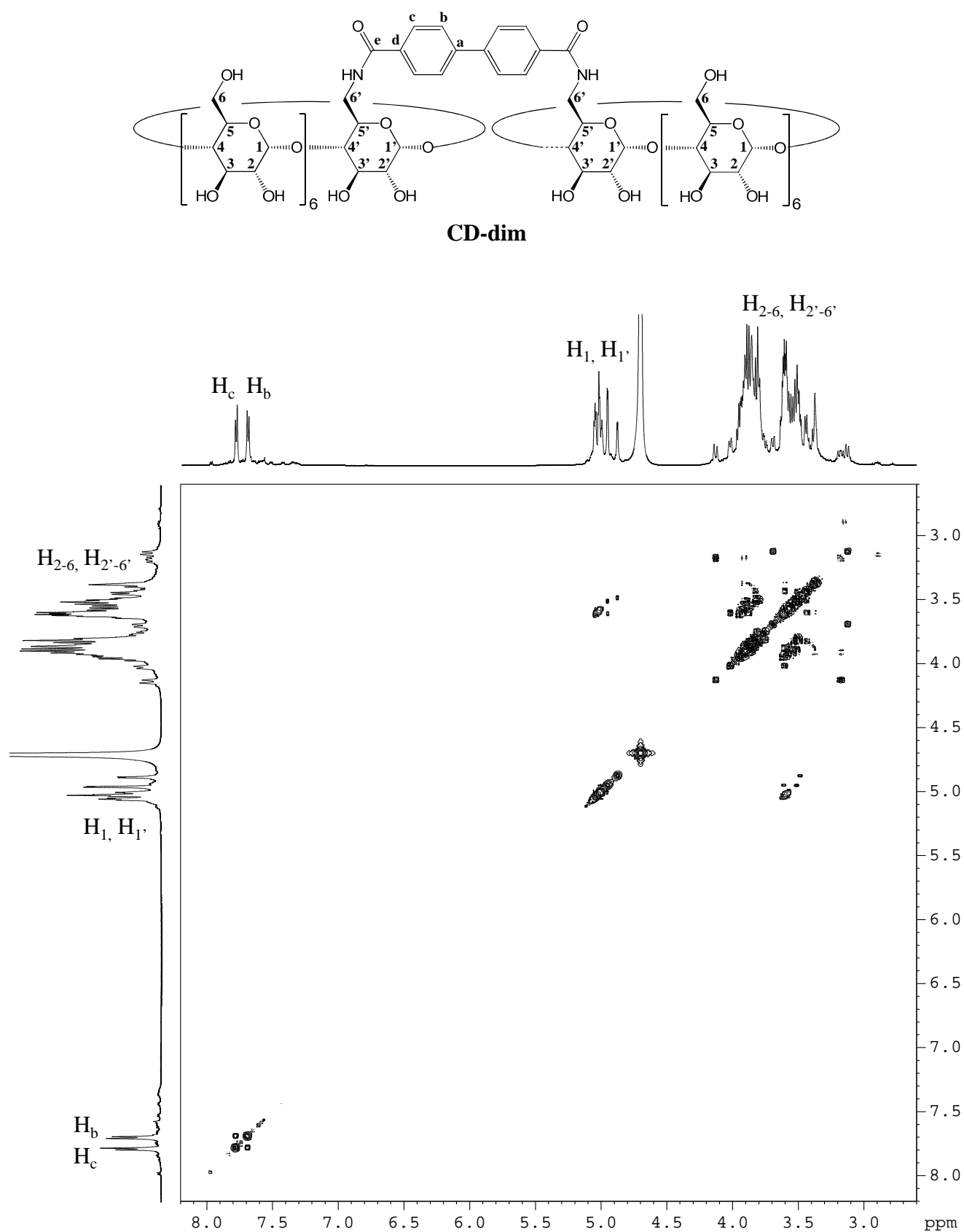


Figure S6: COSY NMR spectrum of *N,N'*-bis[(6^A-deoxy-β-cyclodextrin)yl] biphenyl-4,4'-dicarboxamide (**CD-dim**) (600 MHz, D₂O).

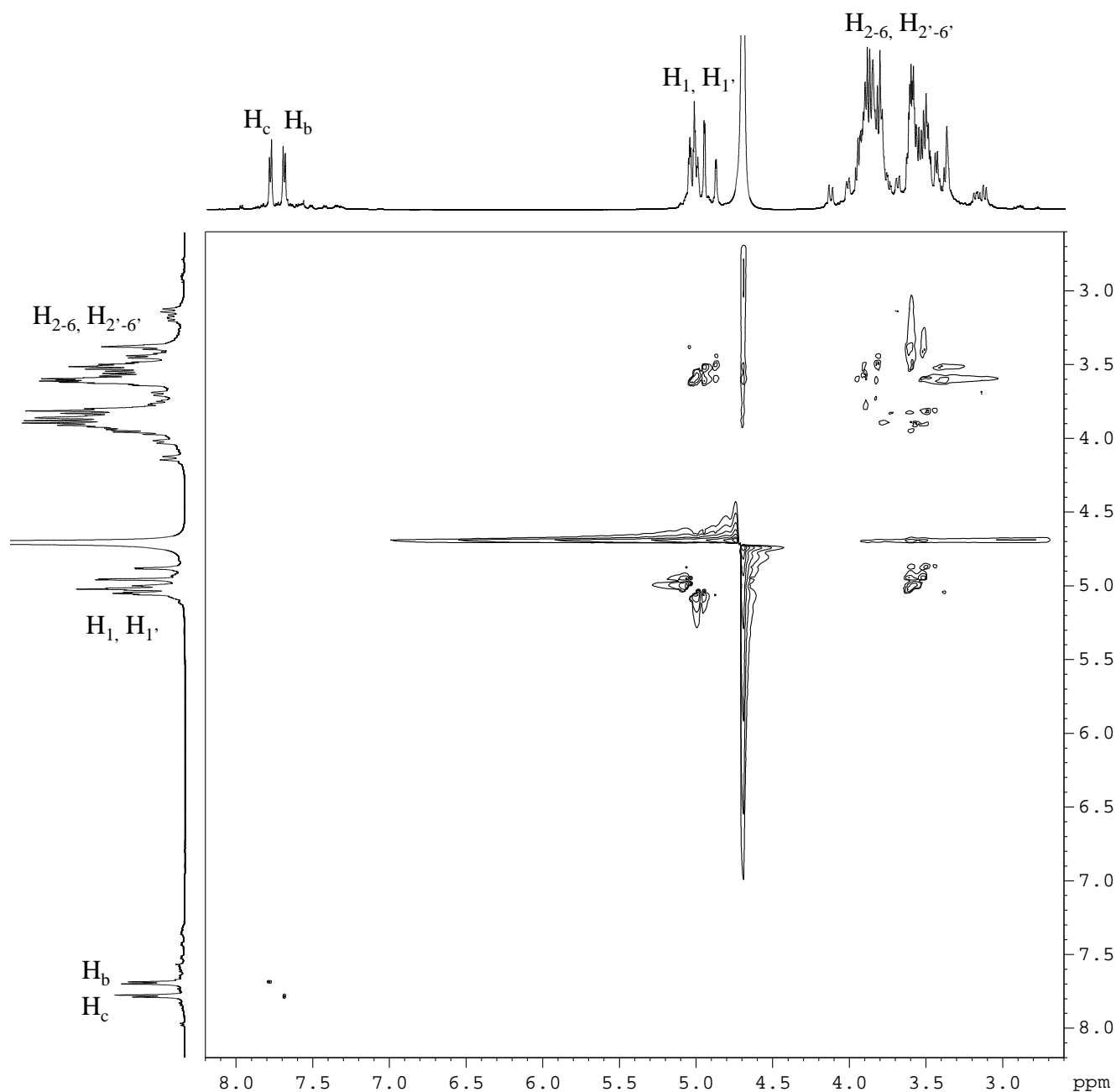
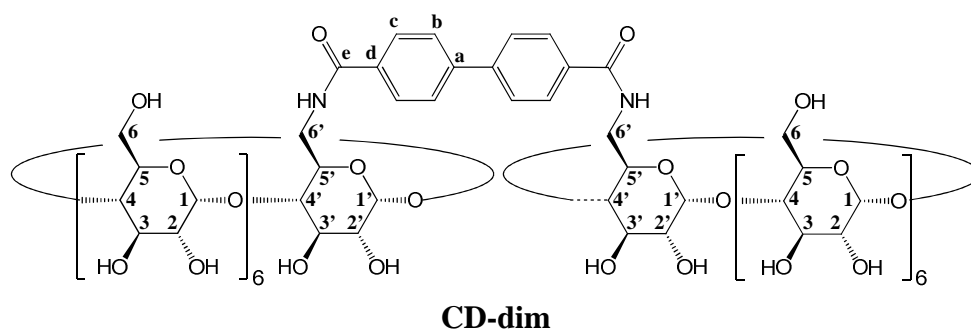


Figure S7: T-ROESY NMR spectrum of *N,N'*-bis[(6^A-deoxy-β-cyclodextrin)yl] biphenyl-4,4'-dicarboxamide (**CD-dim**) (600 MHz, D₂O).

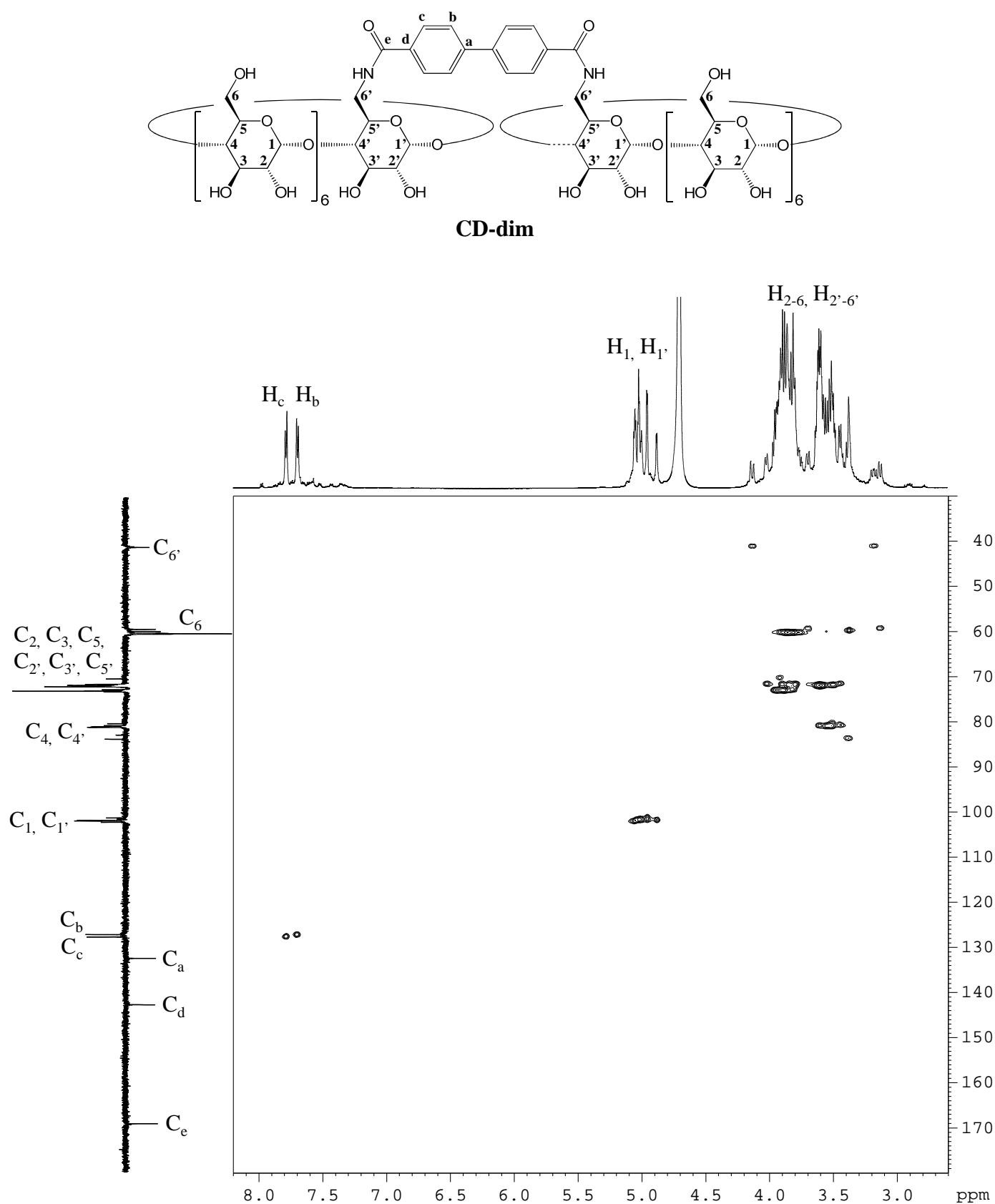


Figure S8: HSQC NMR spectrum of *N,N'*-bis[(6^A-deoxy-β-cyclodextrin)yl] biphenyl-4,4'-dicarboxamide (**CD-dim**) (D₂O).

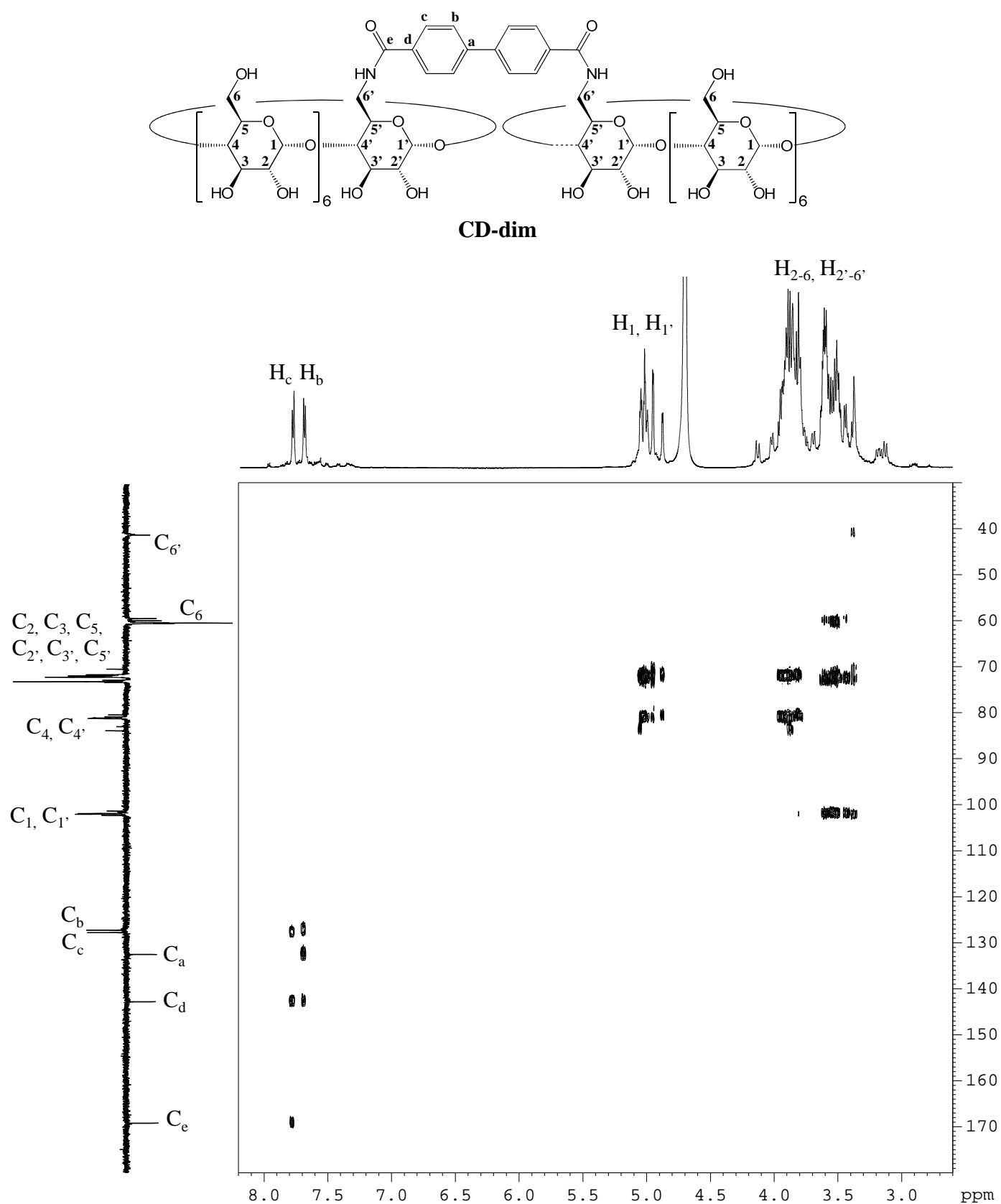
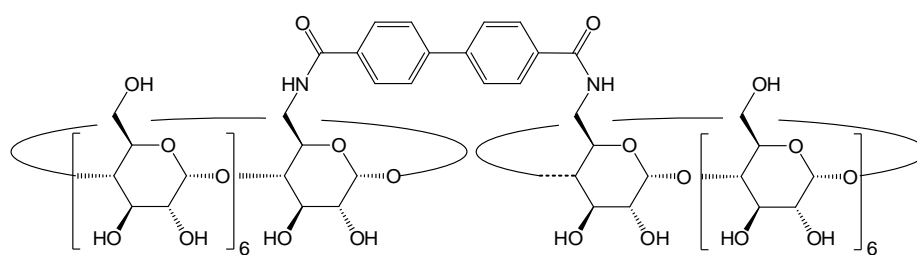


Figure S9: HMBC NMR spectrum of *N,N'*-bis[(6^A-deoxy-β-cyclodextrin)yl] biphenyl-4,4'-dicarboxamide (**CD-dim**) (D₂O).



CD-dim ($C_{98}H_{148}O_{70}N_2$)

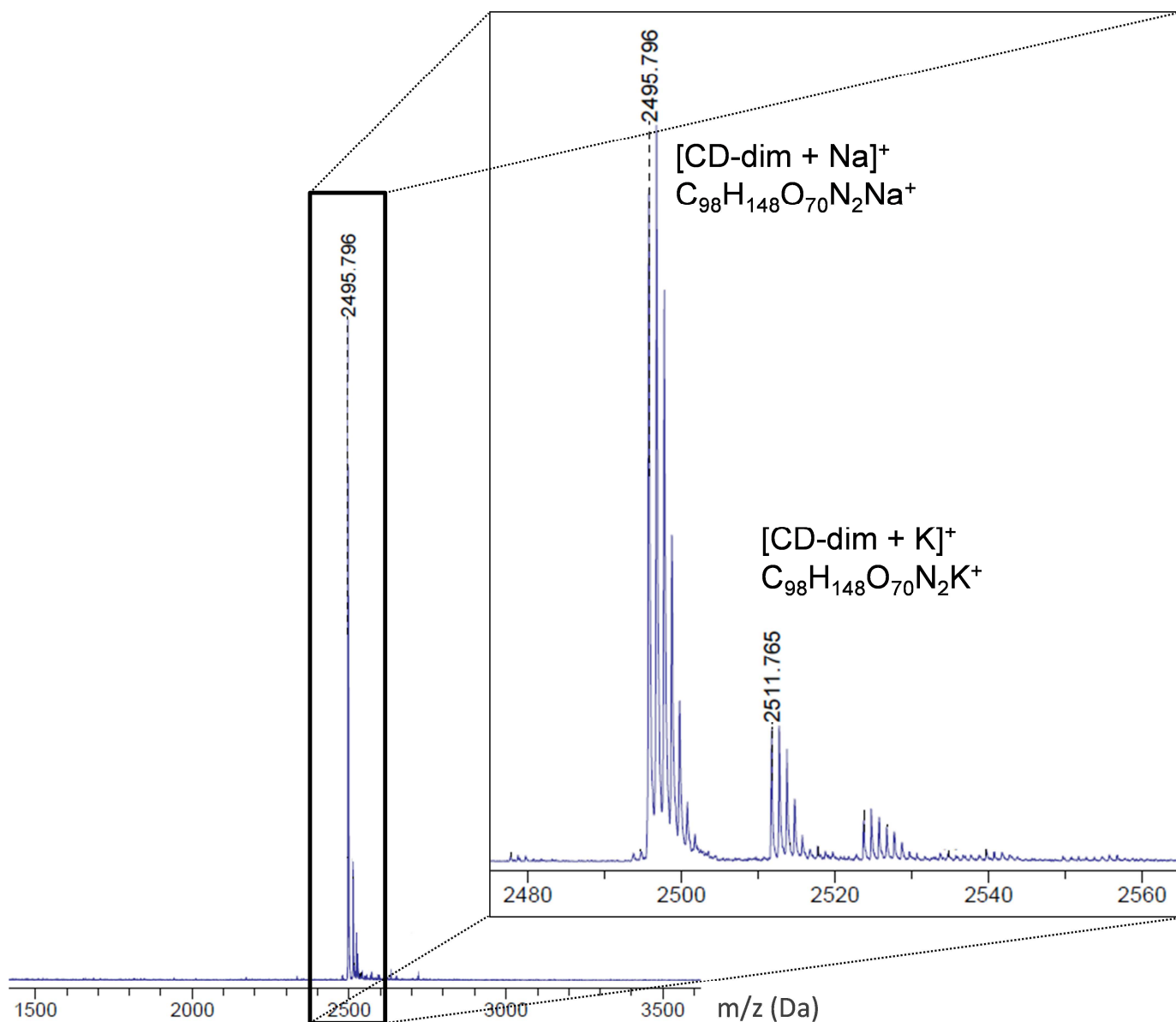


Figure S10: MS MALDI-TOF spectrum of *N,N'*-bis[(6^A-deoxy-β-cyclodextrin)yl] biphenyl-4,4'-dicarboxamide (**CD-dim**): $m/z = 2495.796$ [CD-dim + Na]⁺ (calculated 2495.798), 2511.765 [CD-dim + K]⁺ (calculated 2511.772).

III.3) $[\text{Rh}(\text{COD})(\mathbf{1})_2]^+$, BF_4^- complex

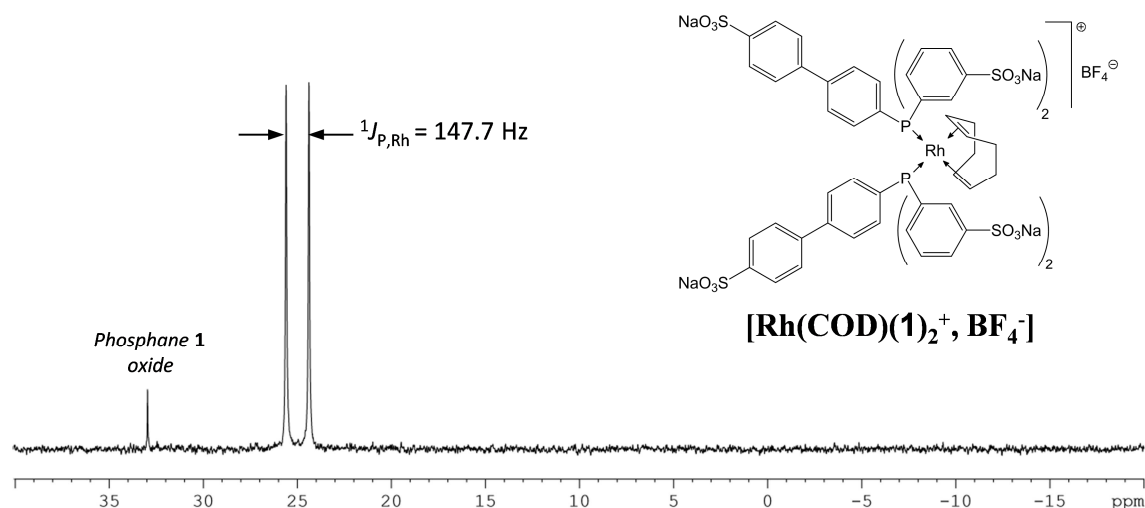


Figure S11: $^{31}\text{P}\{^1\text{H}\}$ NMR spectrum of $[\text{Rh}(\text{COD})(\mathbf{1})_2]^+$, BF_4^- (121.5 MHz, D_2O).

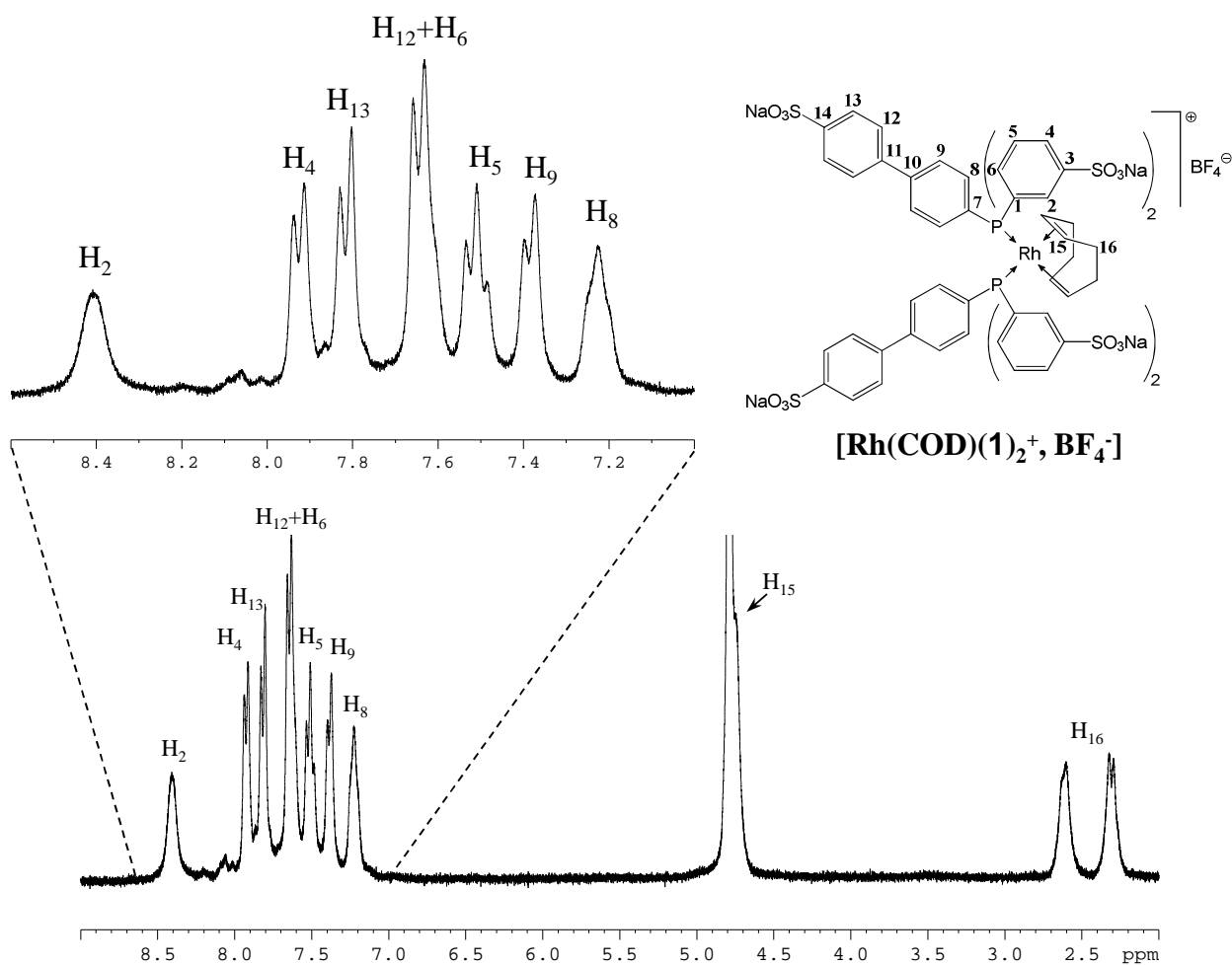


Figure S12: ^1H NMR spectrum of $[\text{Rh}(\text{COD})(\mathbf{1})_2]^+$, BF_4^- (300 MHz, D_2O).

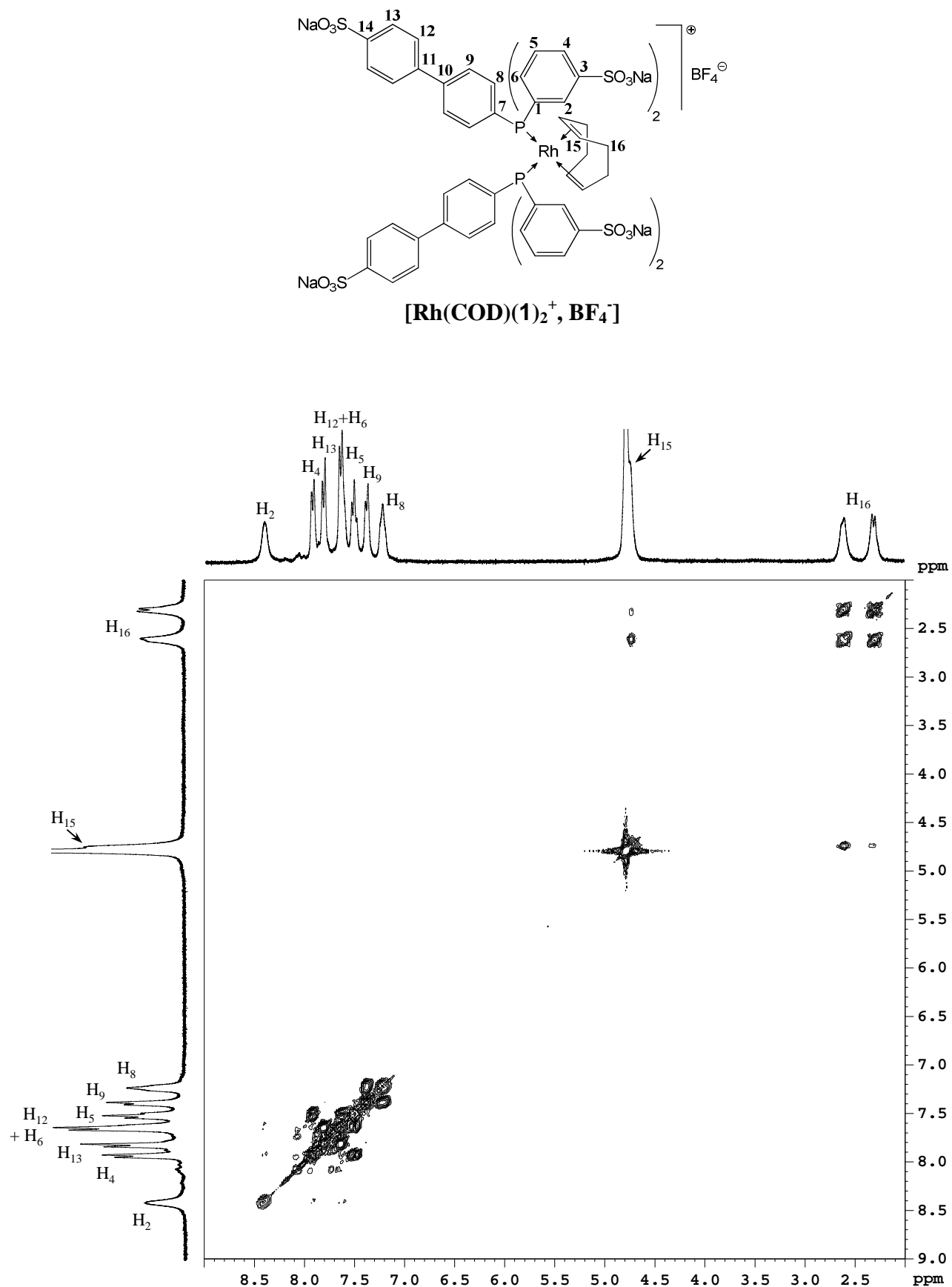


Figure S13: COSY NMR spectrum of $[\text{Rh}(\text{COD})(\mathbf{1})_2]^+$, BF_4^- (300 MHz, D_2O).

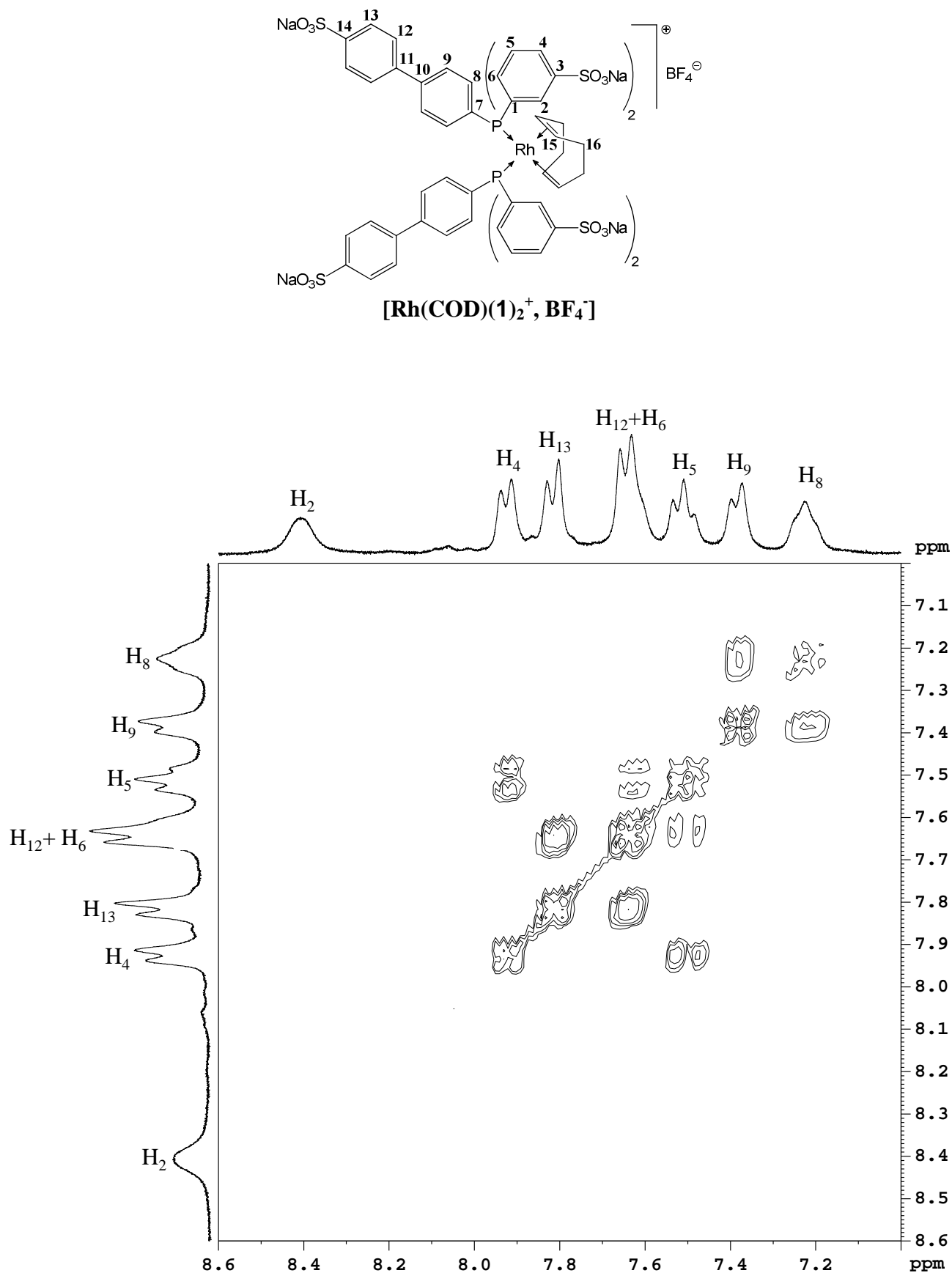


Figure S14: Zoom of COSY NMR spectrum of $[\text{Rh}(\text{COD})(\mathbf{1})_2]^+$, BF_4^- (300 MHz, D_2O).

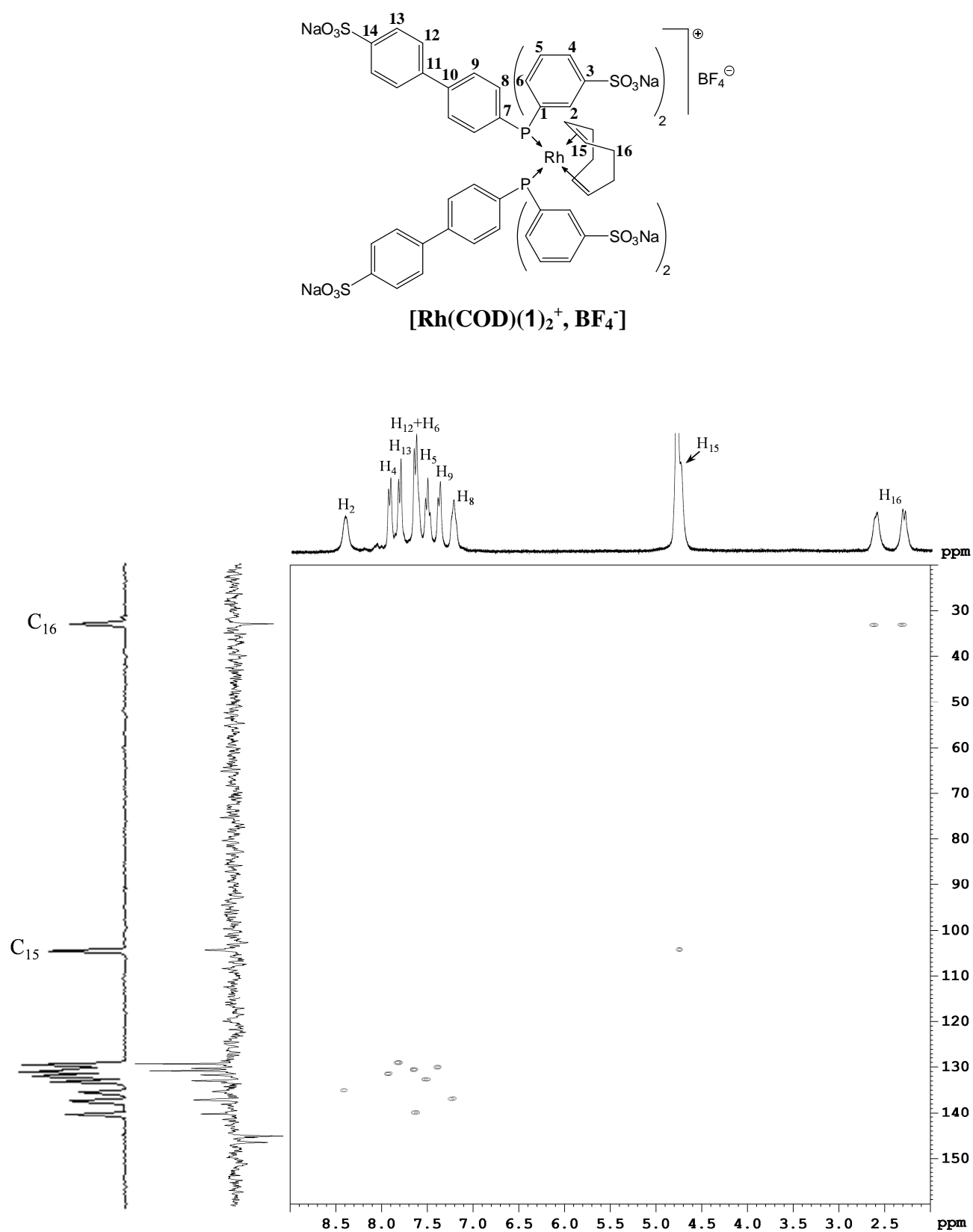


Figure S15: HSQC NMR spectrum of $[\text{Rh}(\text{COD})(\mathbf{1})_2]^+$, BF_4^- (D_2O).

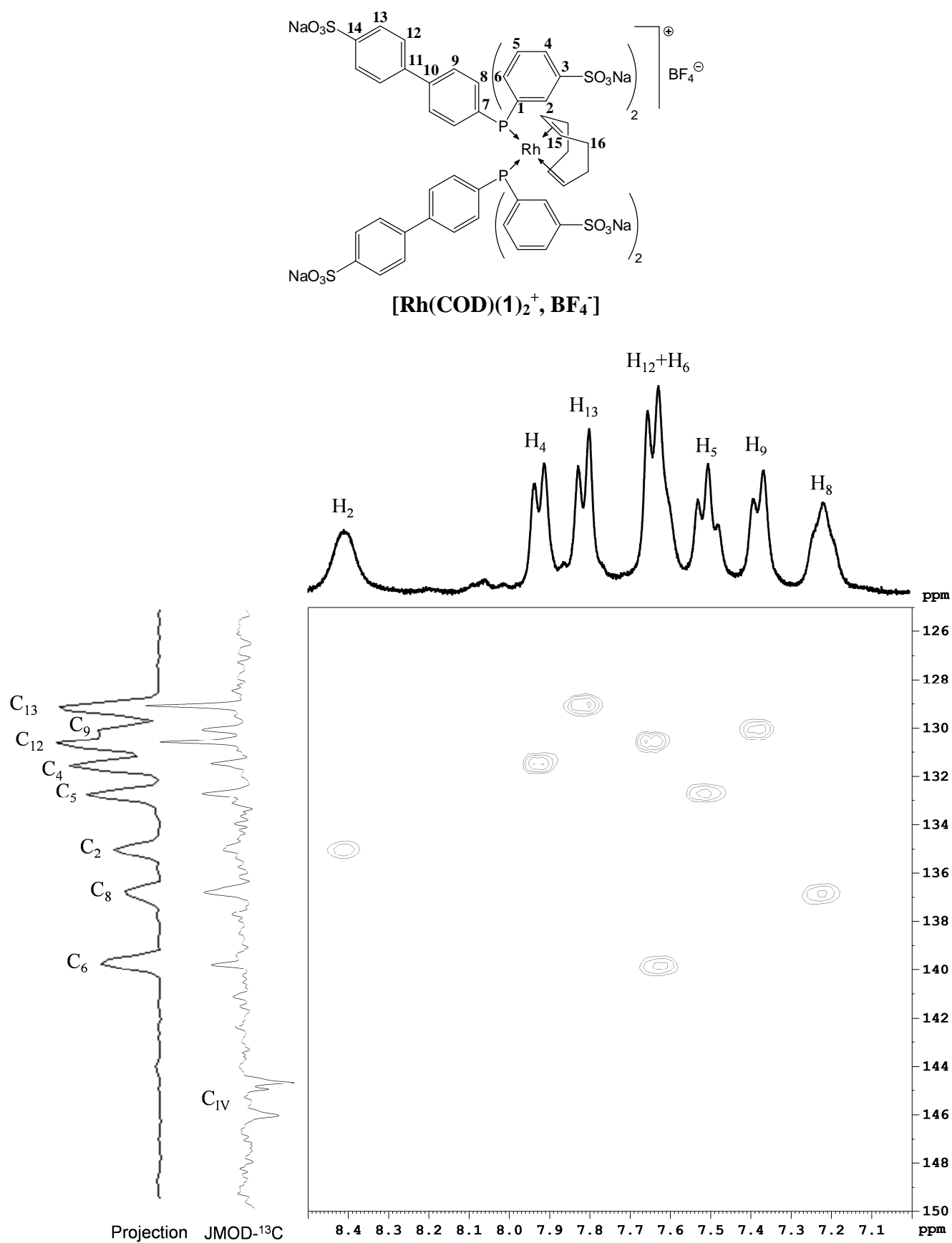


Figure S16: Zoom of HSQC NMR spectrum of $[\text{Rh}(\text{COD})(\mathbf{1})_2]^+$, BF_4^- (D_2O).

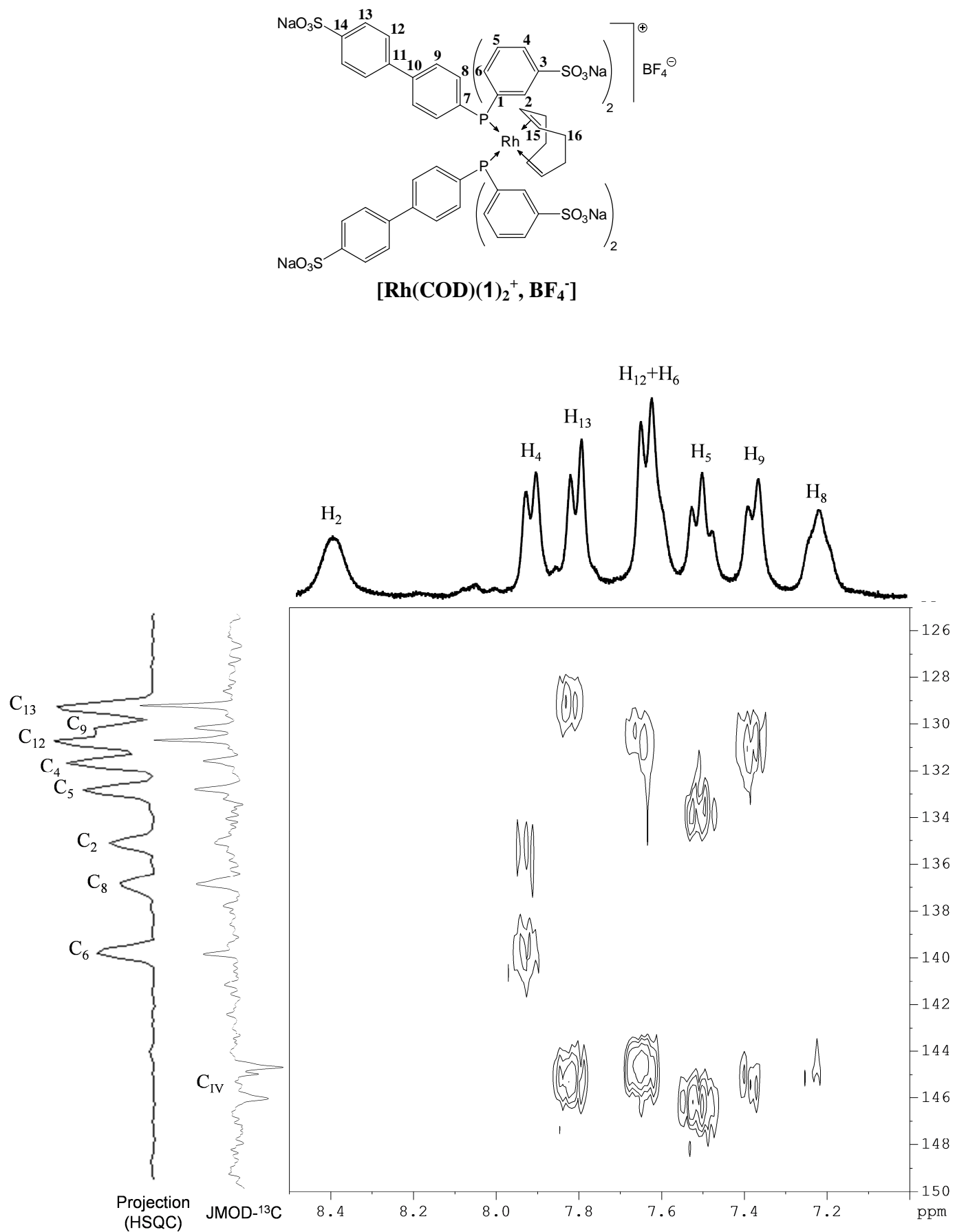


Figure S17: HMBC NMR spectrum of $[\text{Rh}(\text{COD})(\mathbf{1})_2]^+$, BF_4^- (D_2O).

III.4) $[\text{Rh}(\text{COD})(\text{TPPTS})_2]^+, \text{BF}_4^-$ complex

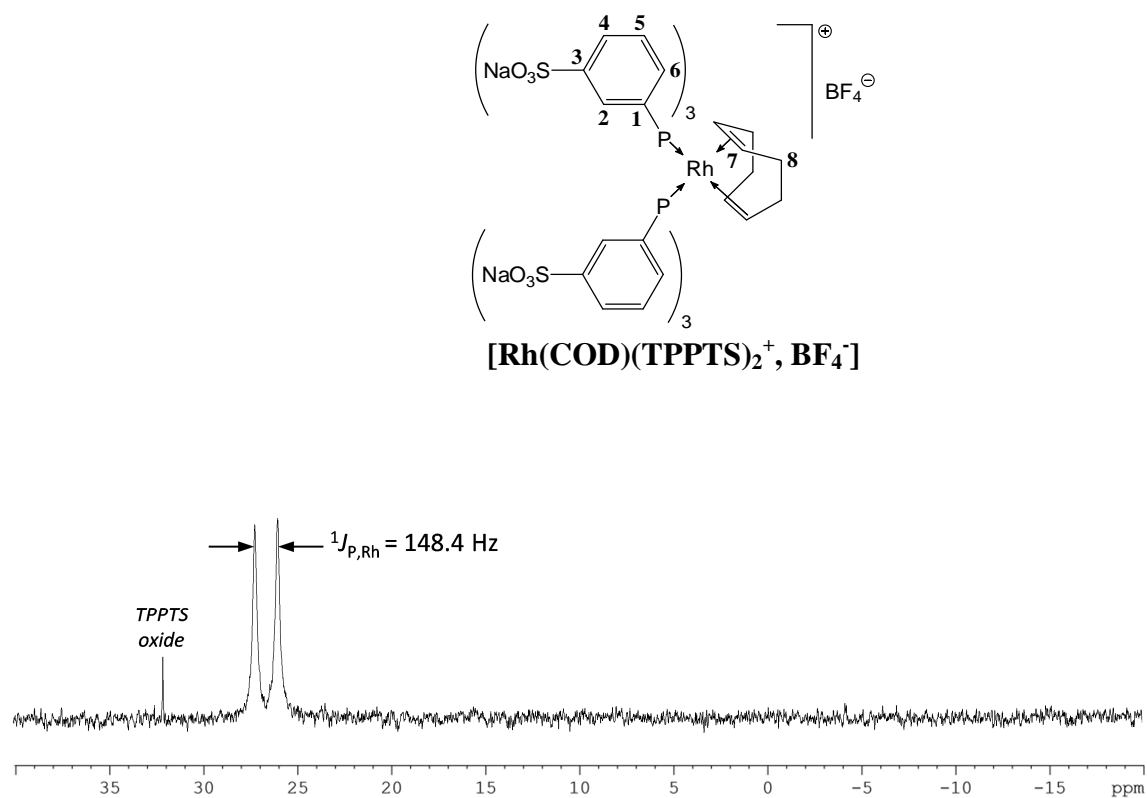


Figure S18: $^{31}\text{P}\{^1\text{H}\}$ NMR spectrum of $[\text{Rh}(\text{COD})(\text{TPPTS})_2]^+, \text{BF}_4^-$ (121.5 MHz, D_2O).

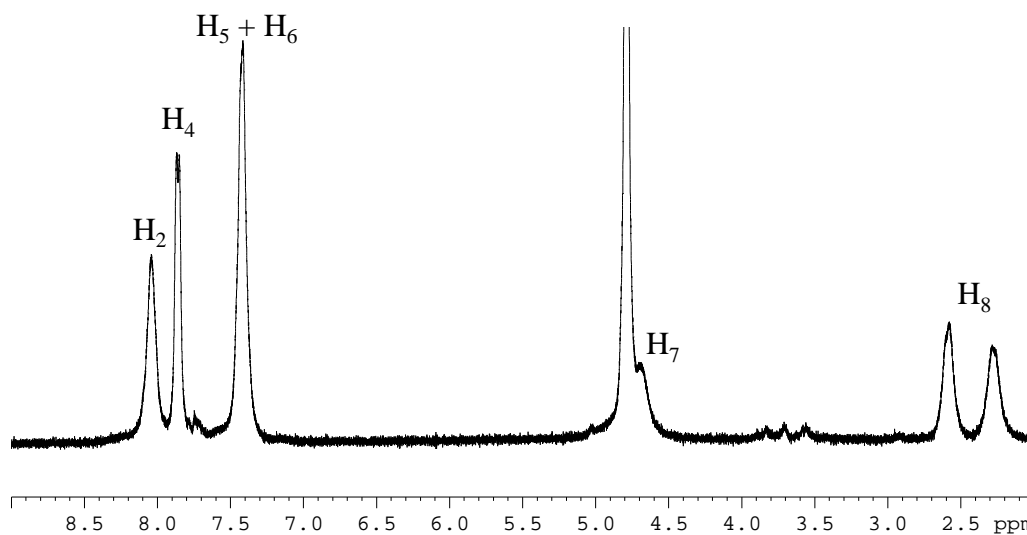


Figure S19: ^1H NMR spectrum of $[\text{Rh}(\text{COD})(\text{TPPTS})_2]^+, \text{BF}_4^-$ (300 MHz, D_2O).

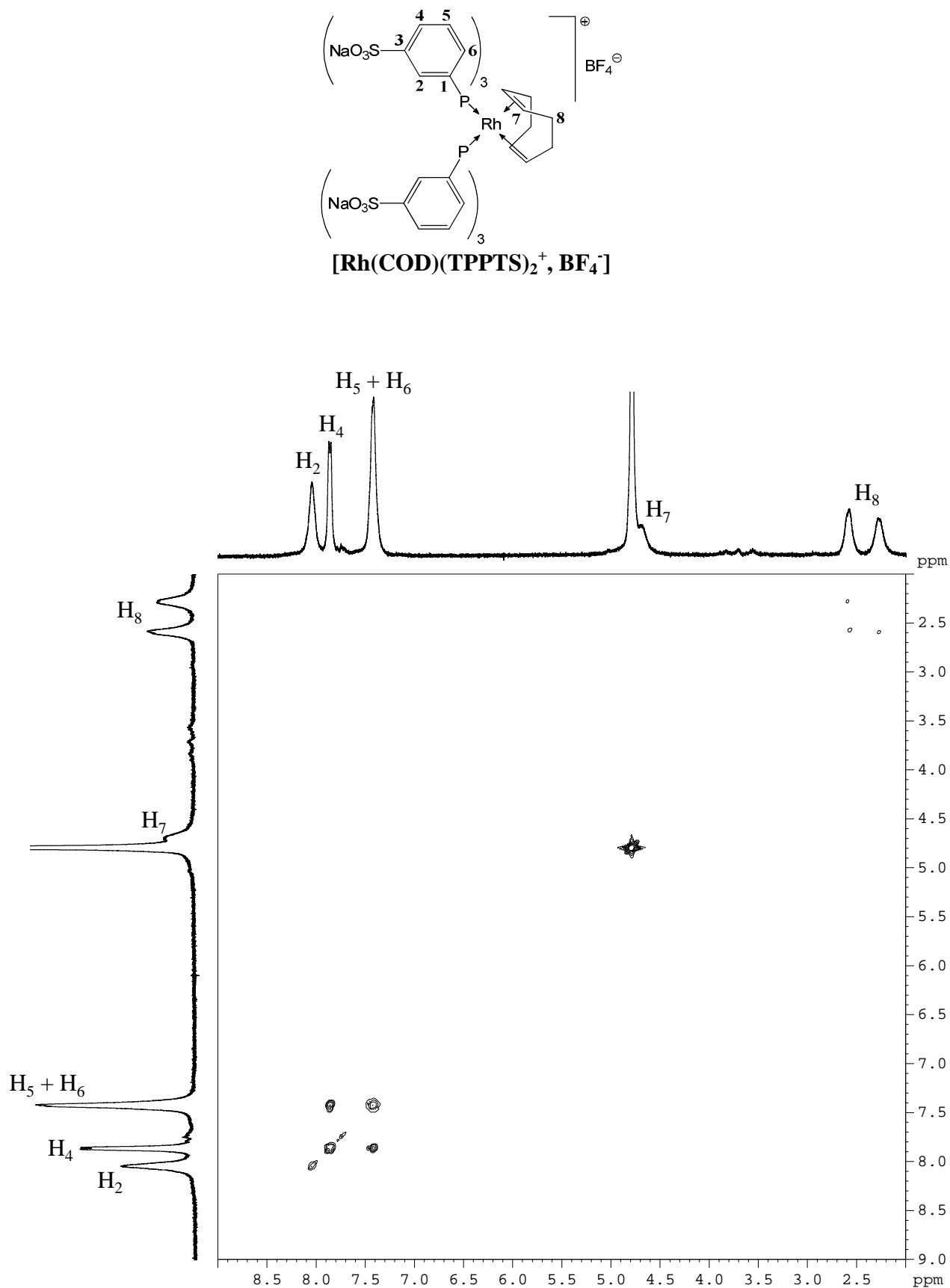


Figure S20: COSY NMR spectrum of **[Rh(COD)(TPPTS)₂⁺, BF₄⁻]** (300 MHz, D₂O).

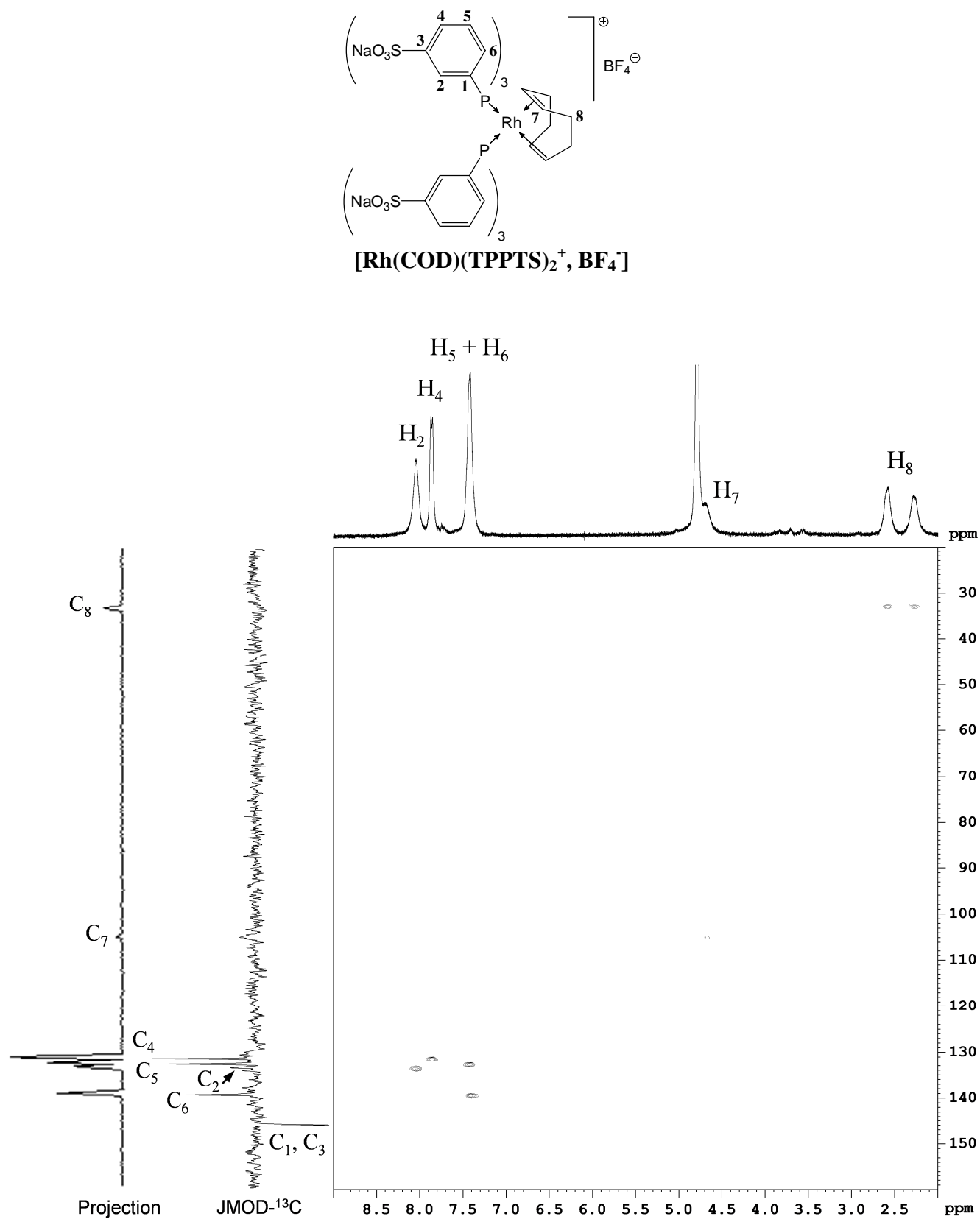


Figure S21: HSQC NMR spectrum of $[\text{Rh}(\text{COD})(\text{TPPTS})_2]^+, \text{BF}_4^-$ (D_2O).

IV) 1D NMR studies of the interactions between the different compounds

IV.1) Evidences of interaction between Phosphane 1 and β -CD

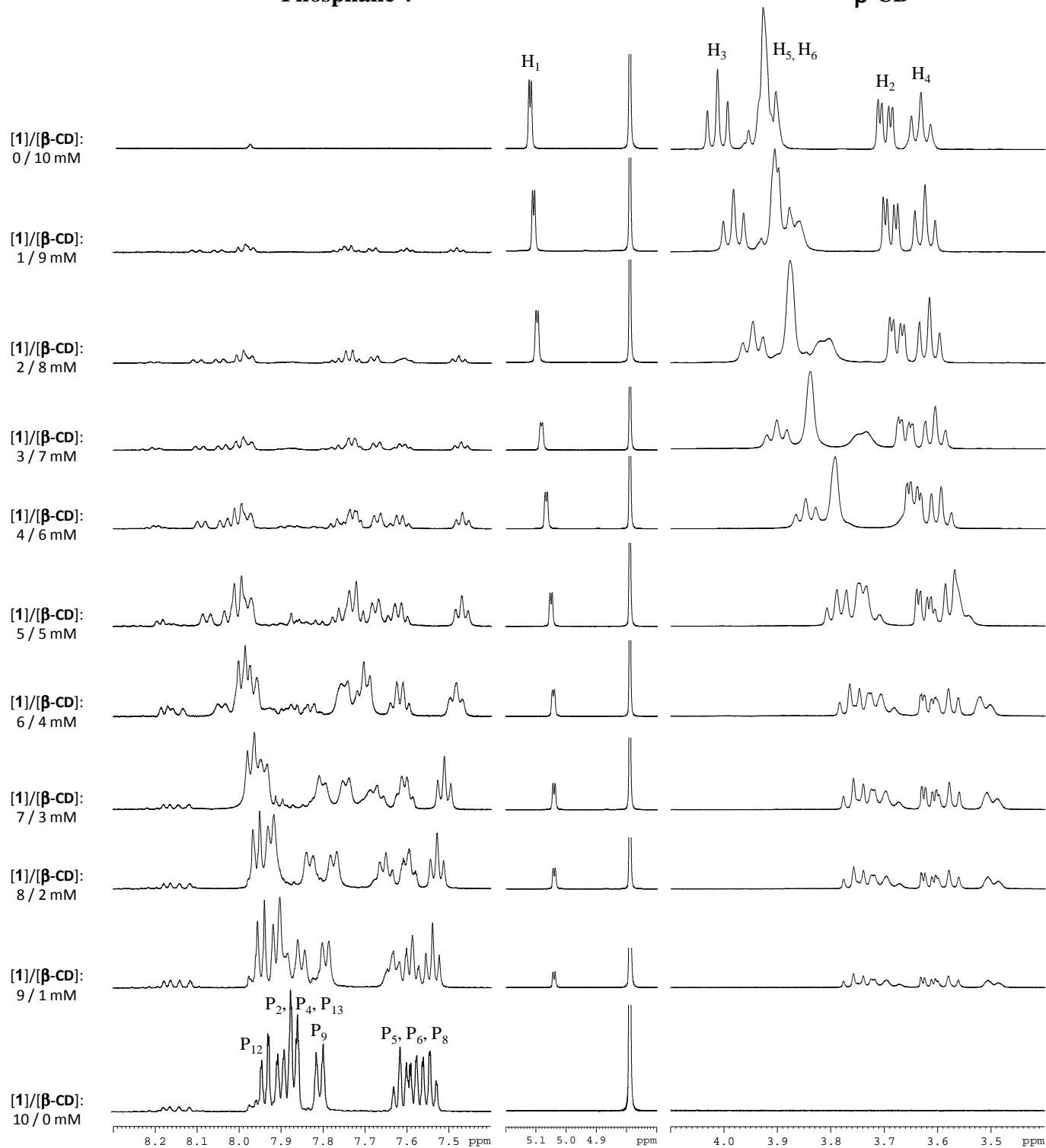
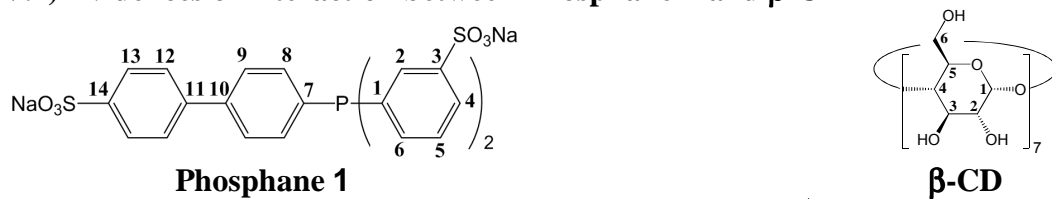


Figure S22: ^1H NMR spectra of Phosphane 1 and β -CD mixtures (500 MHz, D_2O , 20°C)

IV.2) Evidences of interaction between Phosphane 1 and CD-dim

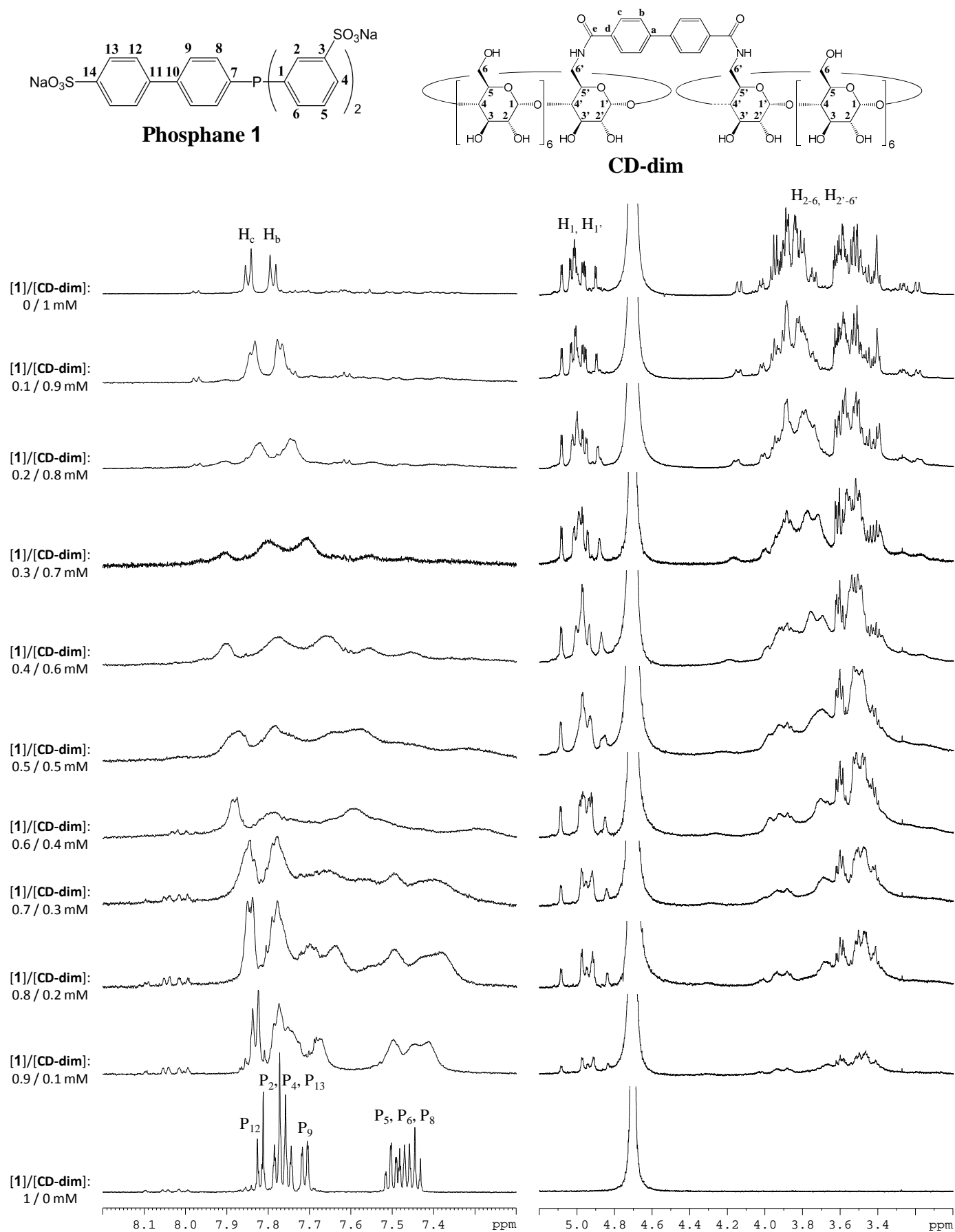


Figure S23: ¹H NMR spectra of **Phosphane 1** and **CD-dim** mixtures (600 MHz, D₂O, 20°C)

IV.3) Evidences of interaction between $[\text{Rh}(\text{COD})(1)_2]^+$, BF_4^- complex and $\beta\text{-CD}$

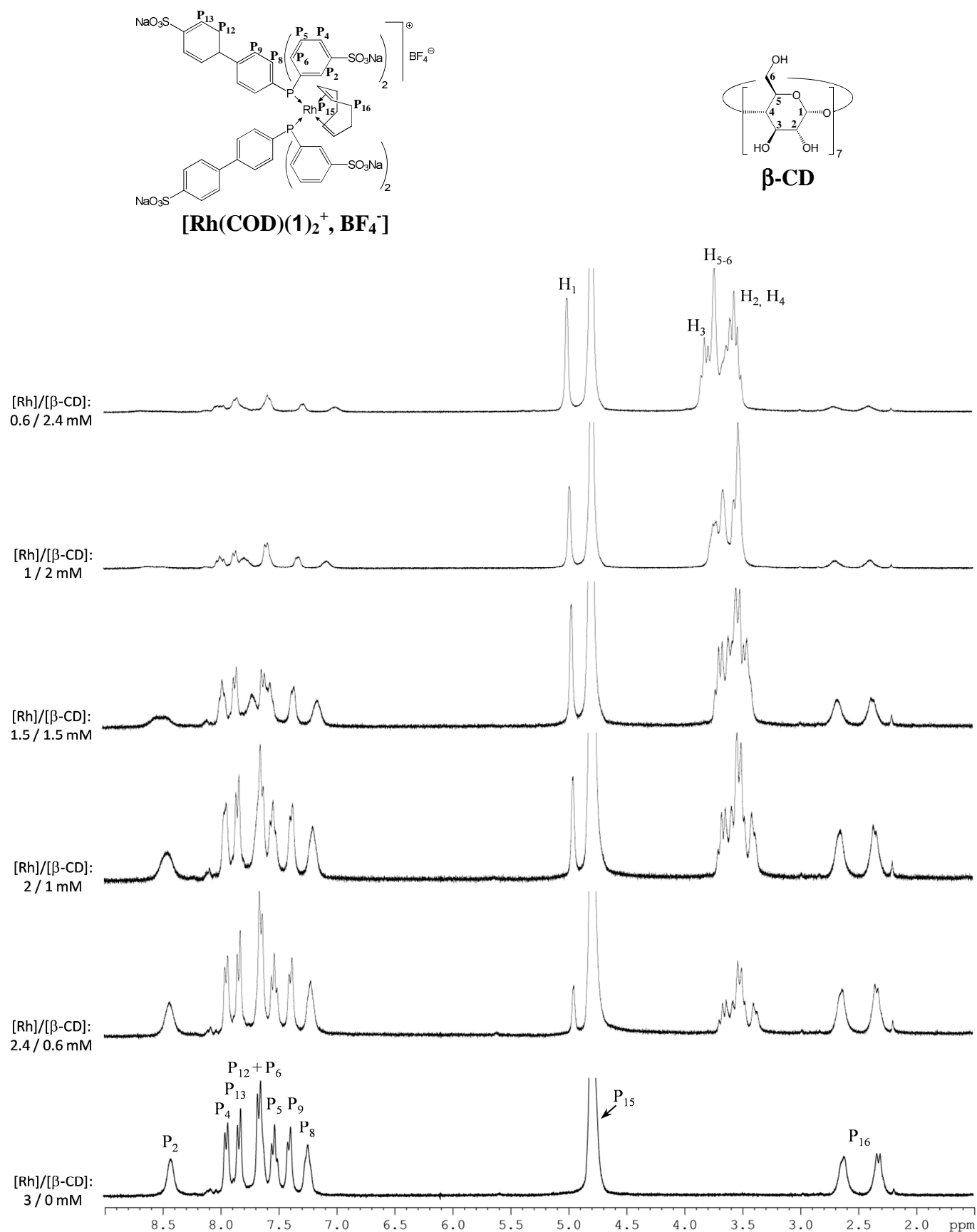


Figure S24: ^1H NMR spectra of $[\text{Rh}(\text{COD})(1)_2]^+$, BF_4^- and $\beta\text{-CD}$ mixtures (300 MHz, D_2O , 20°C)

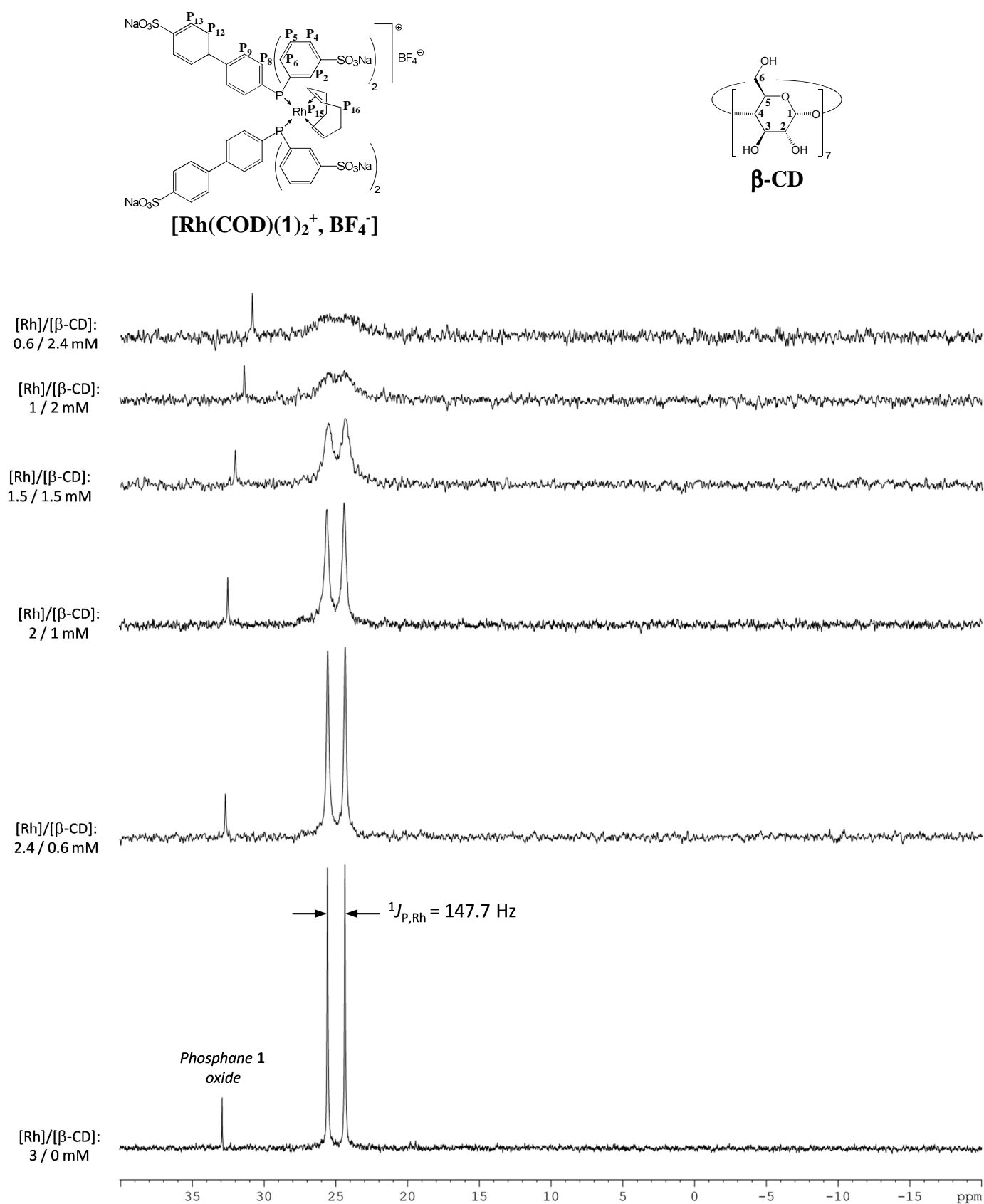


Figure S25: $^{31}\text{P}\{^1\text{H}\}$ NMR spectra of $[\text{Rh}(\text{COD})(\mathbf{1})_2^+, \text{BF}_4^-]$ and $\beta\text{-CD}$ mixtures (121.5 MHz, D_2O , 20°C)

IV.4) Evidences of interaction between $[\text{Rh}(\text{COD})(1)_2^+, \text{BF}_4^-]$ complex and CD-dim

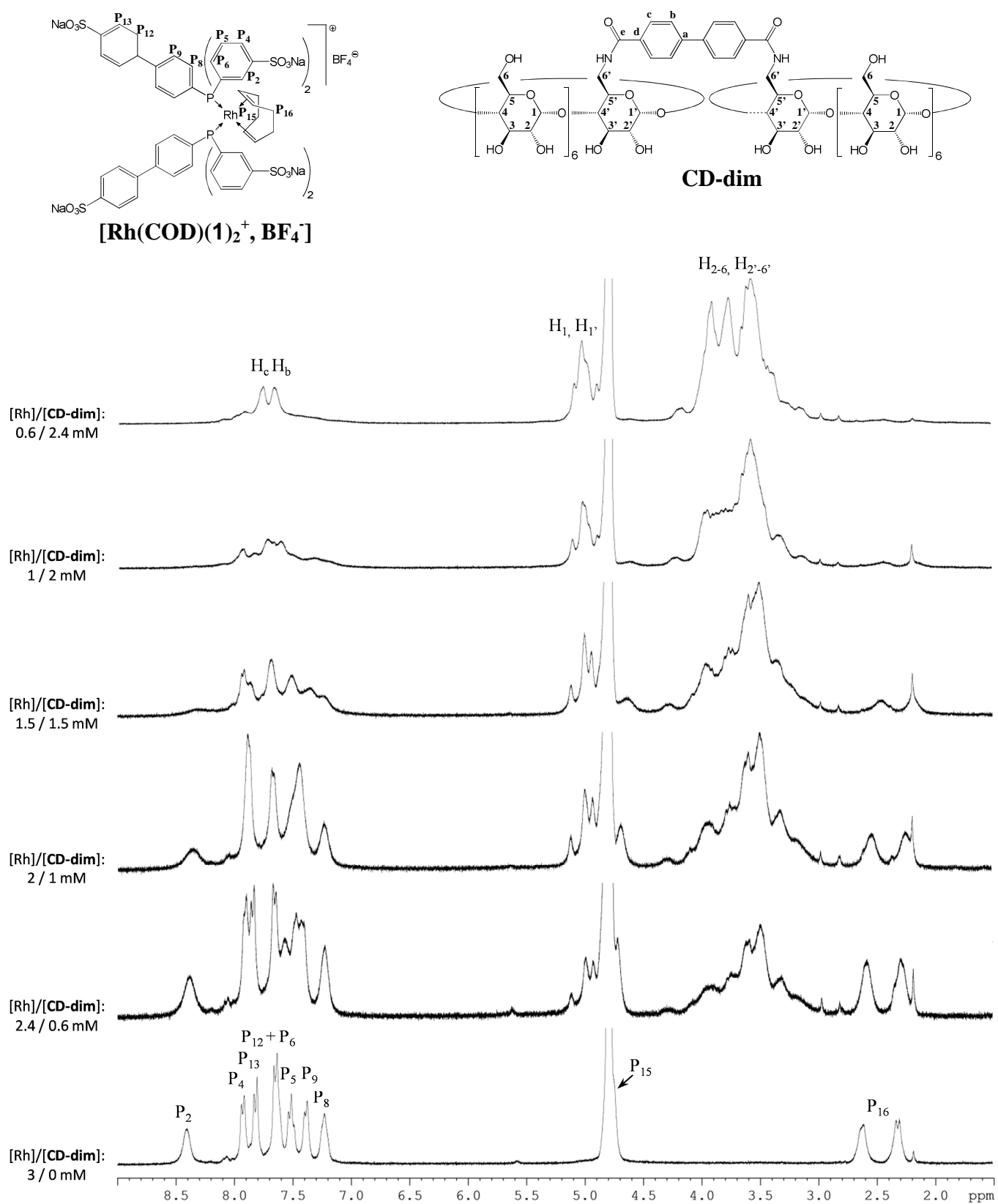


Figure S26: ^1H NMR spectra of $[\text{Rh}(\text{COD})(1)_2^+, \text{BF}_4^-]$ and CD-dim mixtures (300 MHz, D_2O , 20°C)

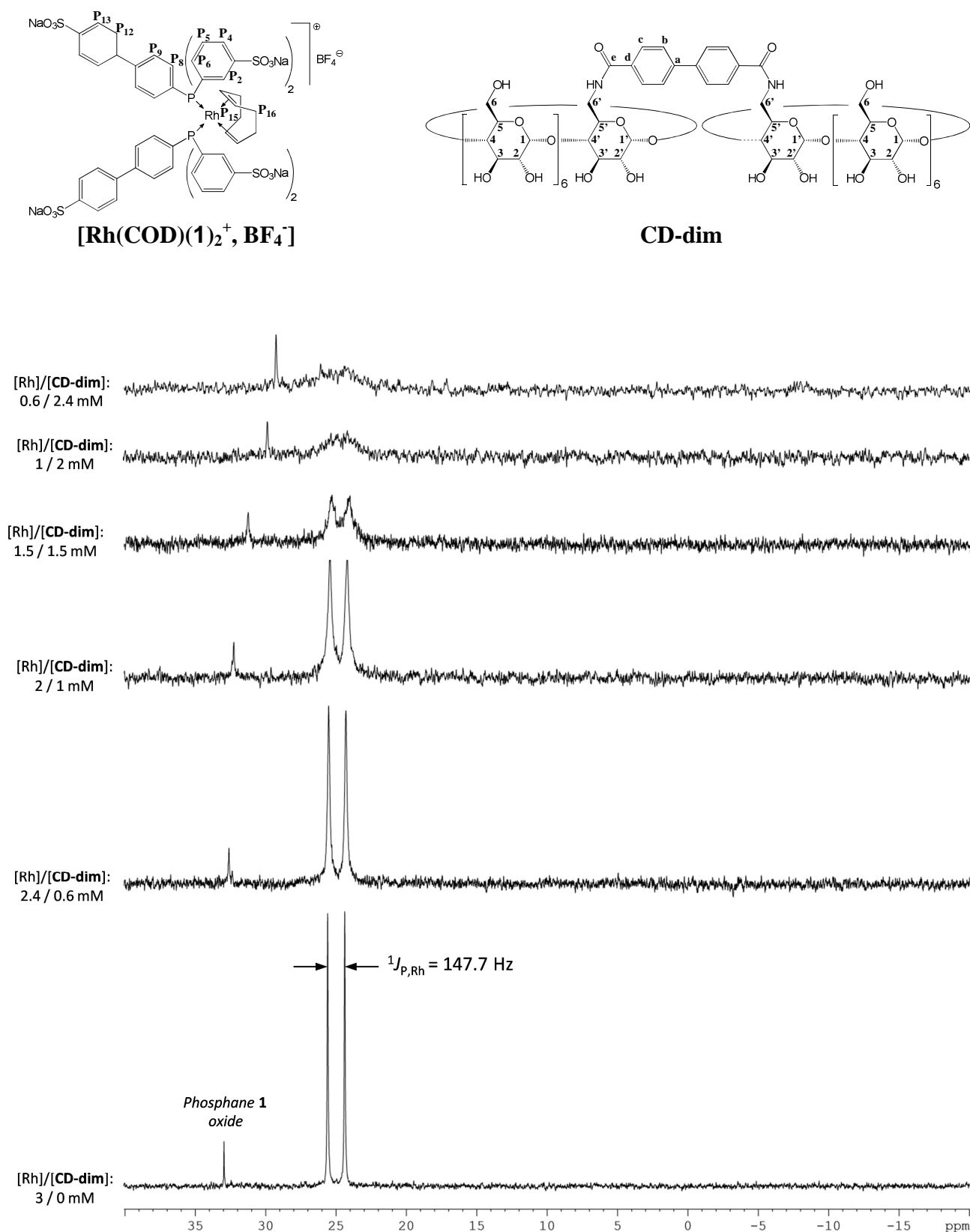


Figure S27: $^{31}\text{P}\{^1\text{H}\}$ NMR spectra of $[\text{Rh}(\text{COD})(1)_2^+, \text{BF}_4^-]$ and CD-dim mixtures
(121.5 MHz, D₂O, 20°C)

IV.5) Evidences of non-interaction between $[\text{Rh}(\text{COD})(\text{TPPTS})_2]^+$, BF_4^- complex and $\beta\text{-CD}/\text{CD-dim}$

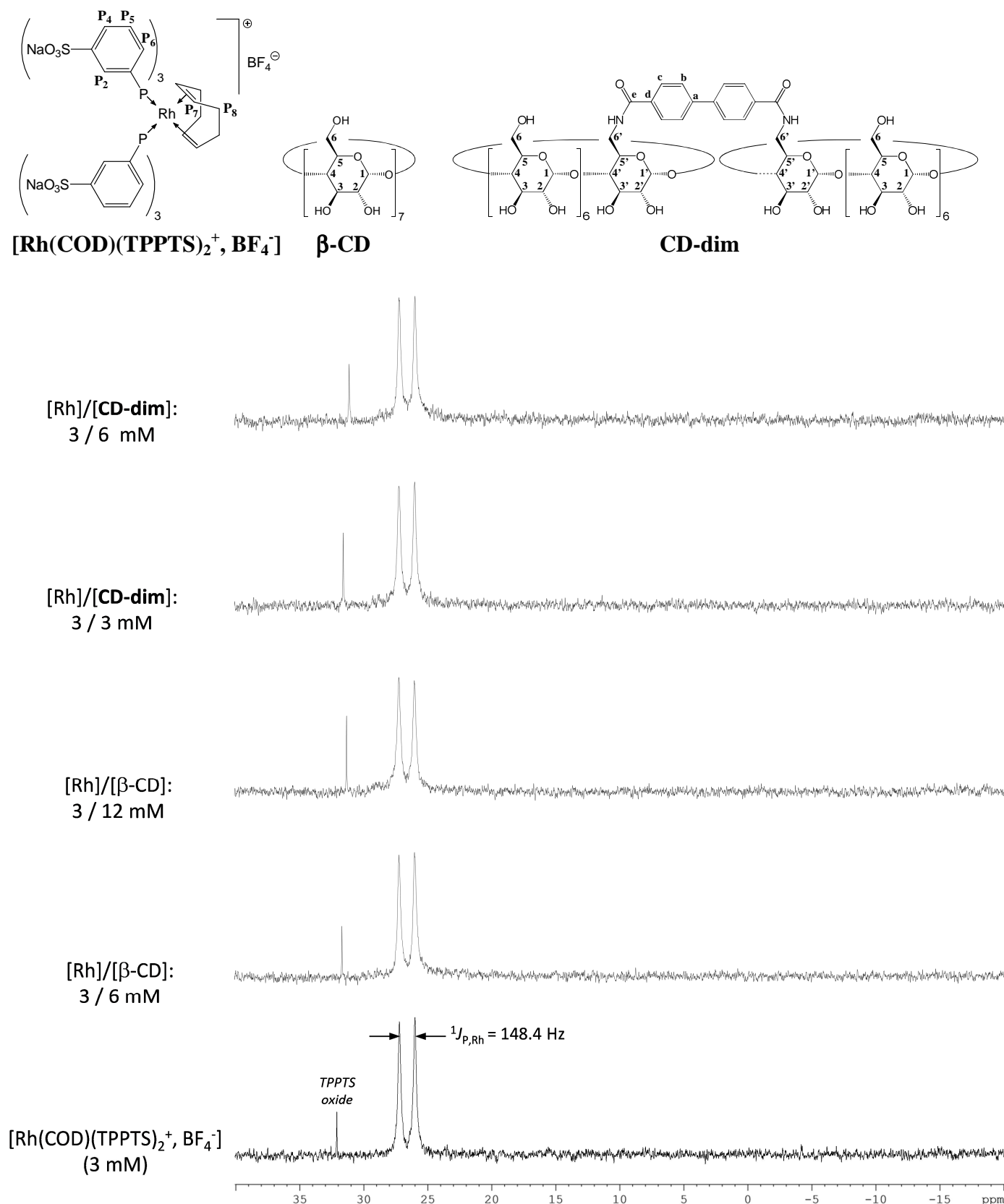


Figure S28: $^{31}\text{P}\{^1\text{H}\}$ NMR spectra of $[\text{Rh}(\text{COD})(\text{TPPTS})_2]^+$, BF_4^- and $\beta\text{-CD}$ or CD-dim mixtures (121.5 MHz, D_2O , 20°C)

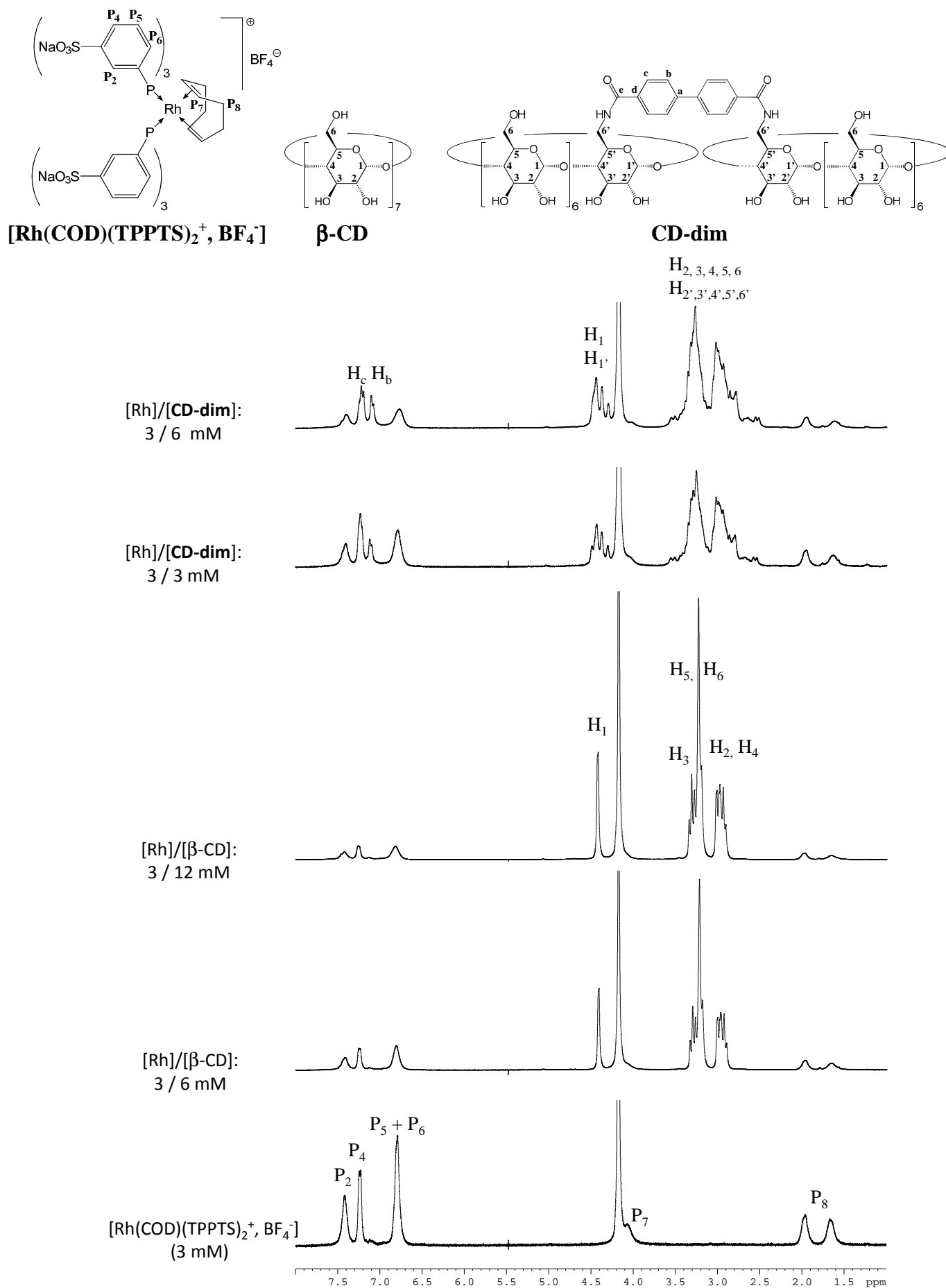


Figure S29: ^1H NMR spectra of $[\text{Rh}(\text{COD})(\text{TPPTS})_2]^+, \text{BF}_4^-$ and $\beta\text{-CD}$ or CD-dim mixtures (300 MHz, D_2O , 20°C)

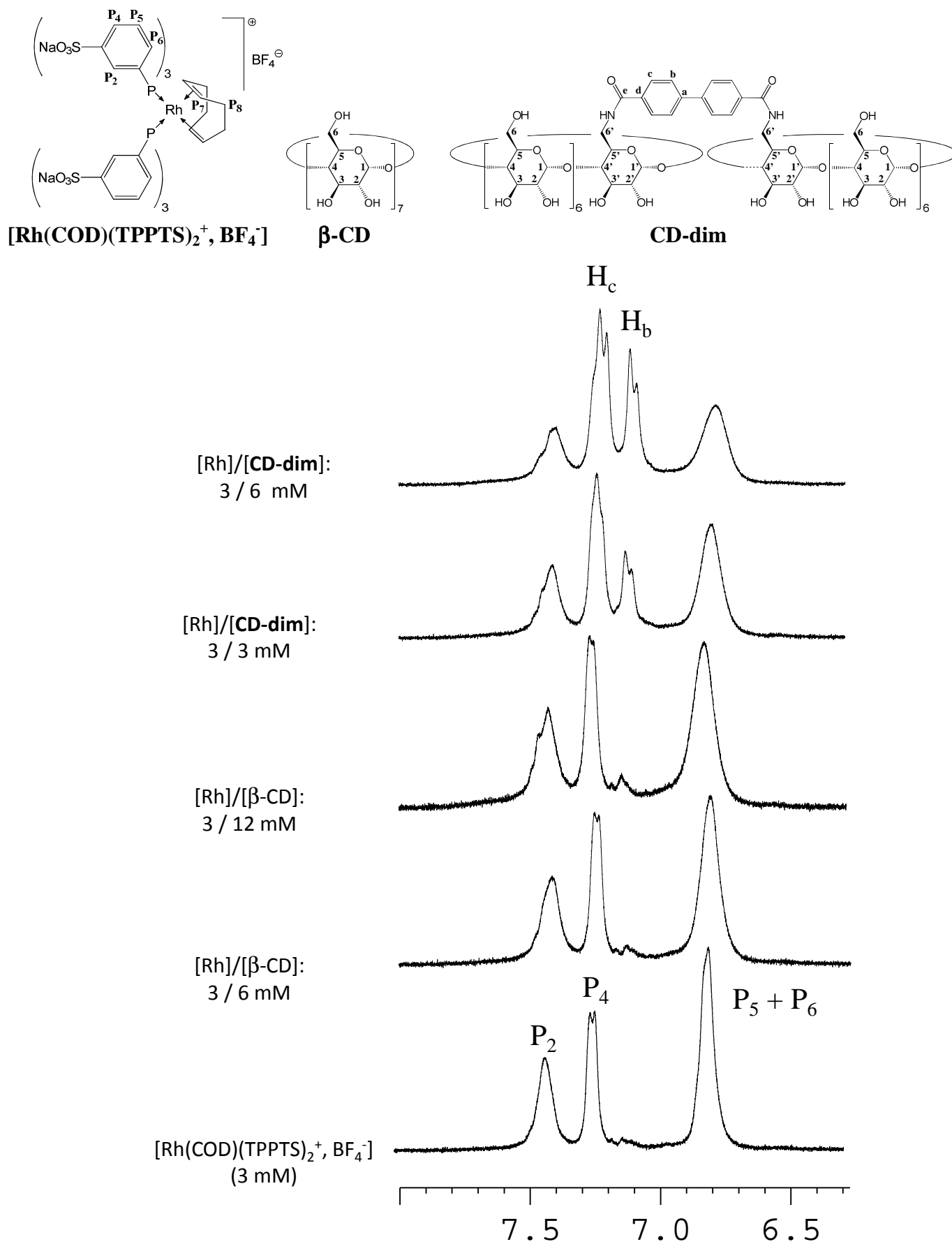


Figure S30: Zooms of ^1H NMR spectra of $[\text{Rh}(\text{COD})(\text{TPPTS})_2]^+$, BF_4^- and $\beta\text{-CD}$ or CD-dim mixtures (300MHz, D_2O , 20°C)

V) Inclusion complexes stoichiometry and association constants

Table S1: “CD derivative:Phosphane” stoichiometries of the inclusion complexes and association constants

	Phosphane 1	TPPTS	$[\text{Rh}(\text{COD})(1)_2^+, \text{BF}_4^-]$	$[\text{Rh}(\text{COD})(\text{TPPTS})_2^+, \text{BF}_4^-]$
β-CD	1:1 ($9\,900\text{ M}^{-1}$)	1:1 ($1\,200\text{ M}^{-1}$) ^[a]	2:1 ^[b]	no interaction
CD-dim	1:2 ($14\,100\text{ M}^{-1}$) ^[c]	1:1 ($1\,740\text{ M}^{-1}$)	1:1	no interaction

^[a] Ferreira M., Bricout H., Sayede A., Ponchel A., Fourmentin S., Tilloy S., Monflier E., Adv. Synth. Catal. 2008, 350, 609 – 618.

^[b] Two β -CD are associated with one $[\text{Rh}(\text{COD})(1)_2^+, \text{BF}_4^-]$. ^[c] One CD-dim is associated with two Phosphanes 1; $K_{11} = K_{12} = 14\,100\text{ M}^{-1}$.

V.1) Interaction between phosphane 1 and β -CD

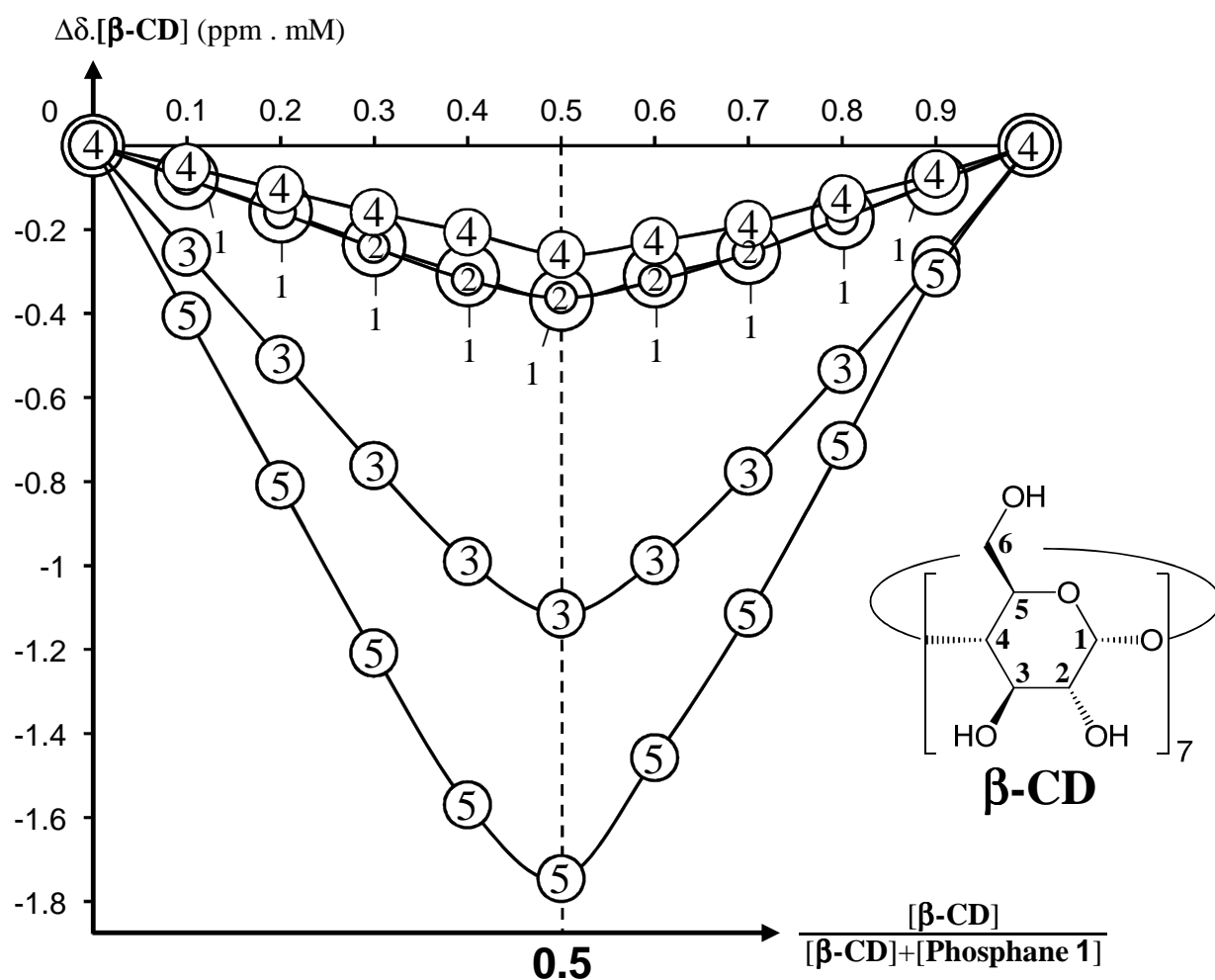


Figure S31: ^1H NMR Job's plot for the combination β -CD : Phosphane 1 (β -CD protons; $[\beta\text{-CD}] + [\text{Phosphane 1}] = 10\text{mM}$ in D_2O , 20°C).

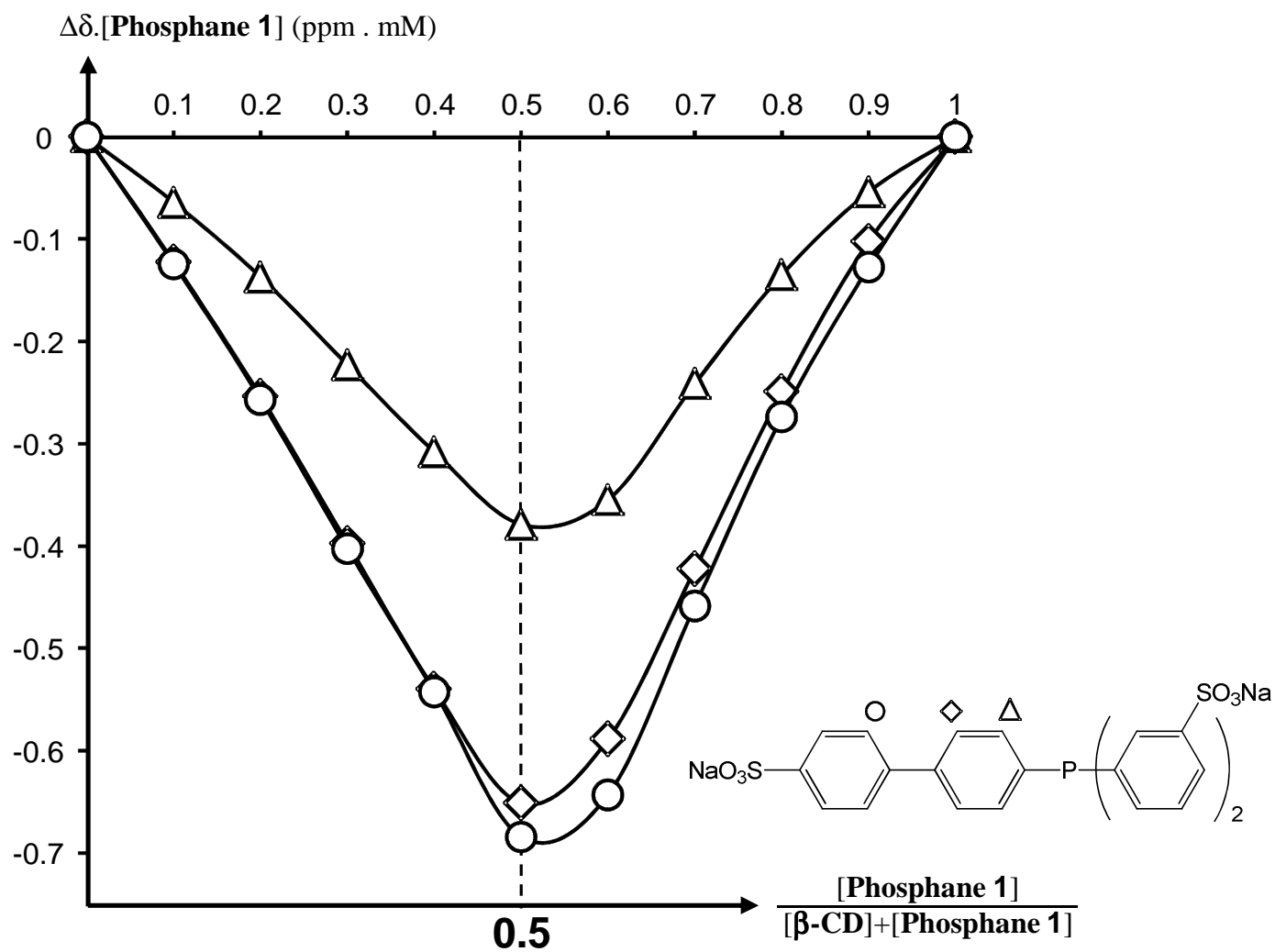


Figure S32: ^1H NMR Job's plot for the combination $\beta\text{-CD}$: **Phosphane 1**
(Phosphane protons; $[\beta\text{-CD}] + [\text{Phosphane 1}] = 10 \text{ mM}$ in D_2O , 20°C).

V.2) Interaction between phosphane 1 and CD-dim

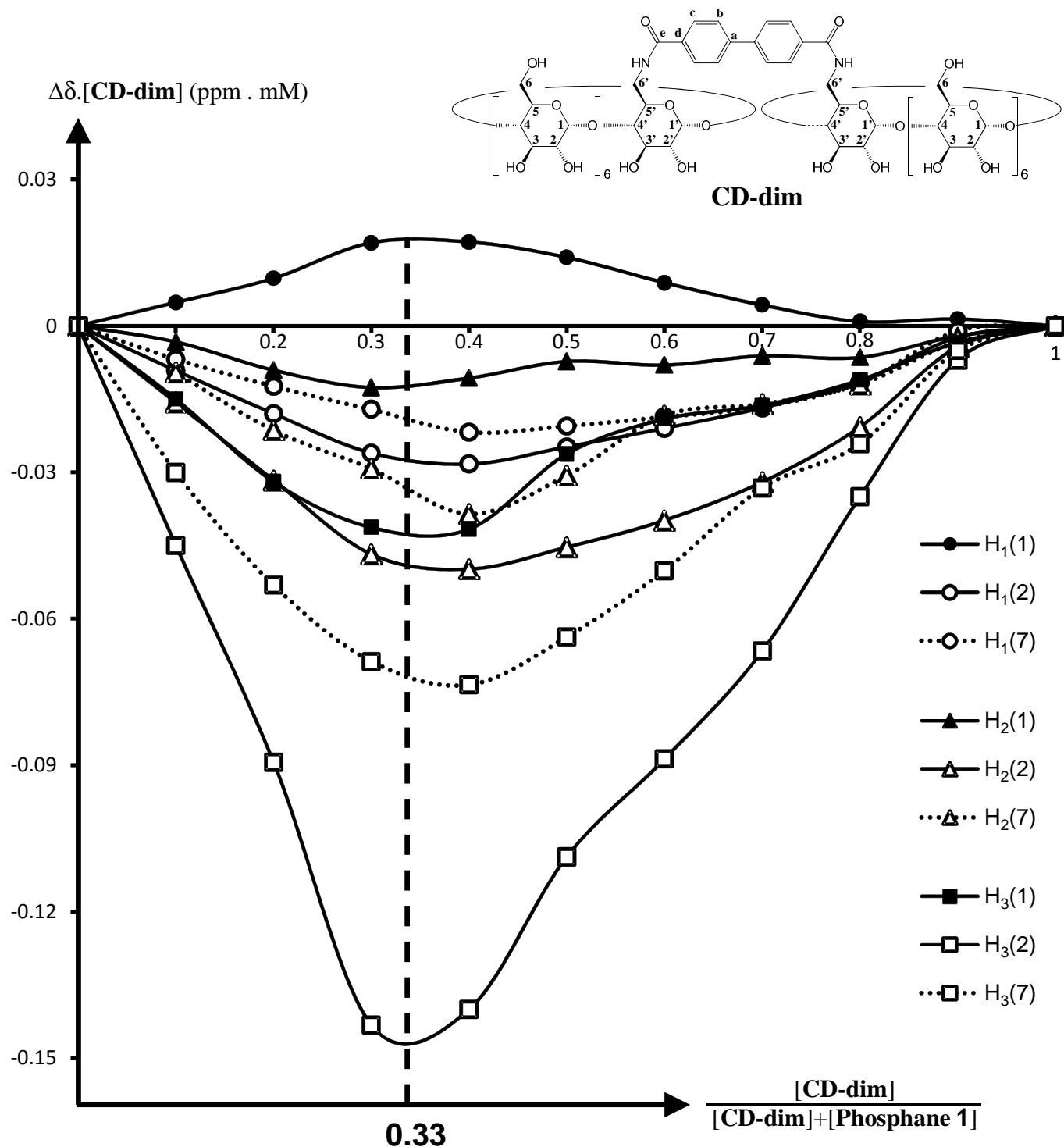


Figure S33: ^1H NMR Job's plot for the combination **CD-dim : Phosphane 1** (CD-dim protons: H_1 , H_2 and H_3 , (1) and (7) correspond respectively to the more and to the less deblinded proton in the initial spectrum of CD-Dim); $[\text{CD-dim}] + [\text{Phosphane 1}] = 1 \text{ mM}$ in D_2O , 20°C).

V.3) Interaction between $[\text{Rh}(\text{COD})(1)_2]^+$, BF_4^- complex and $\beta\text{-CD}$

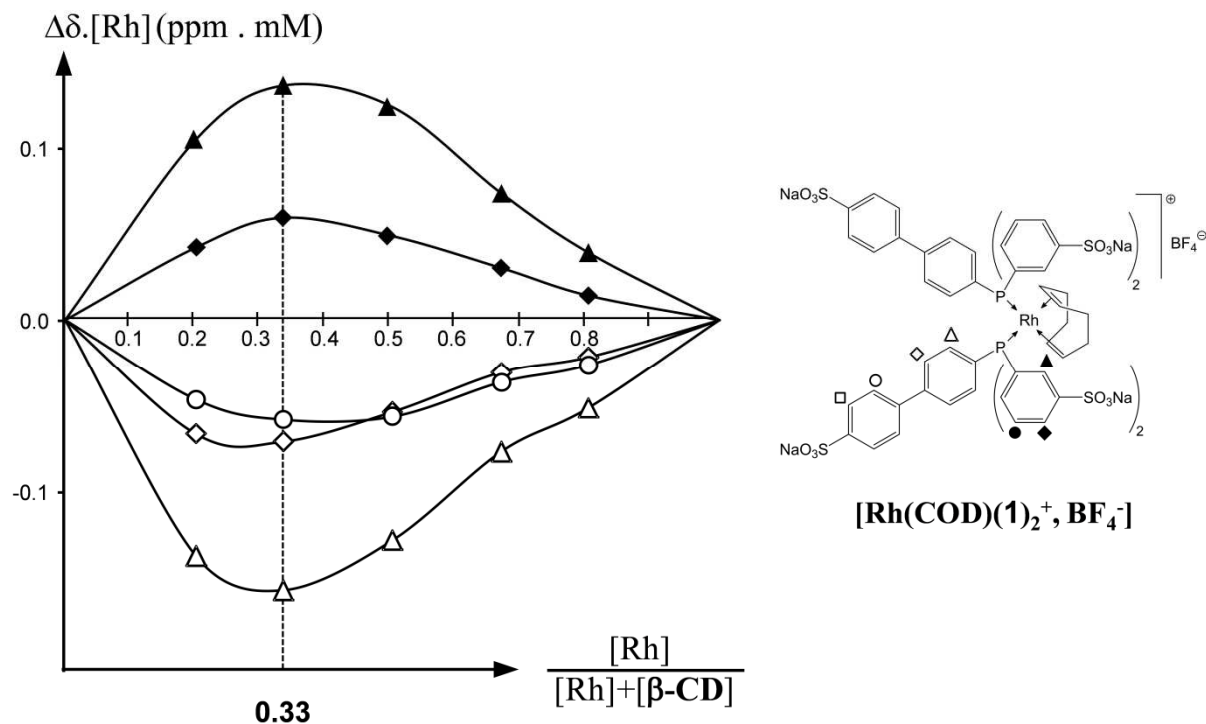


Figure S34: ^1H NMR Job's plot for the combination $\beta\text{-CD} : [\text{Rh}(\text{COD})(1)_2^+, \text{BF}_4^-]$ (Phosphane protons; $[\beta\text{-CD}] + [\text{Rh}] = 3 \text{ mM}$ in D_2O , 20°C).

V.4) Interaction between $[\text{Rh}(\text{COD})(1)_2]^+$, BF_4^- complex and CD-dim

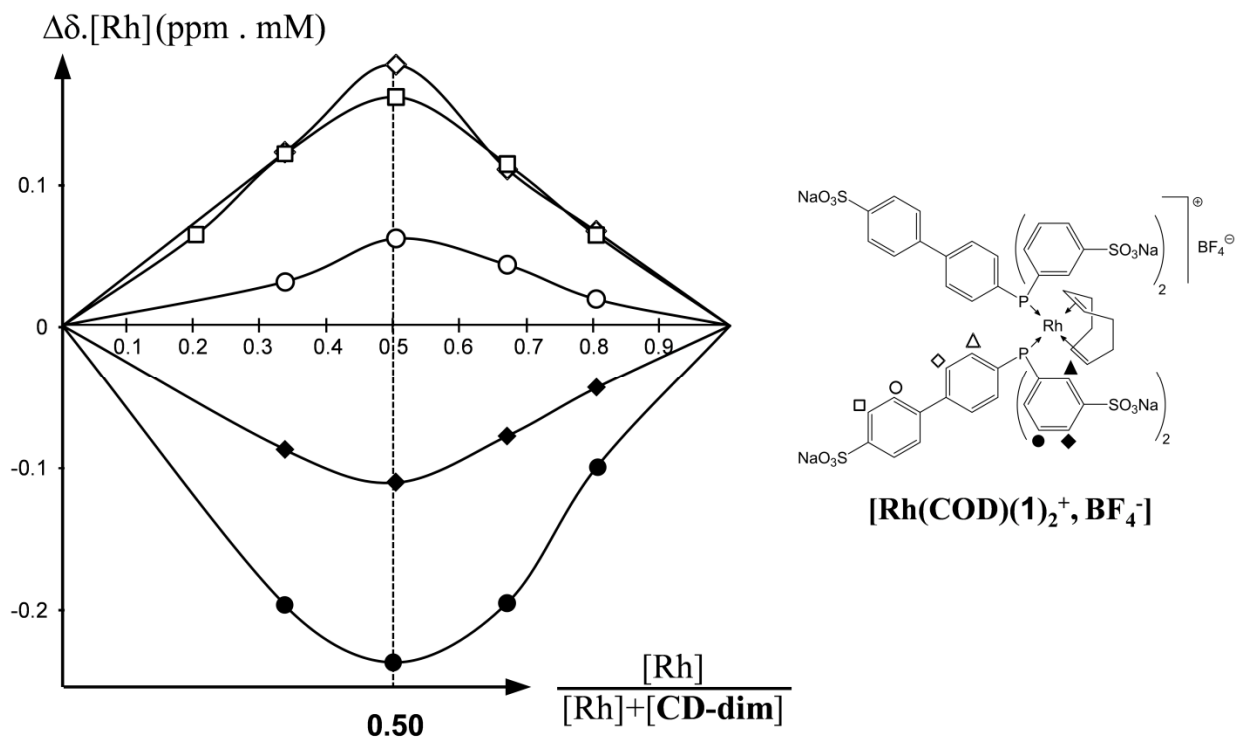


Figure S35: ^1H NMR Job's plot for the combination $\text{CD-dim} : [\text{Rh}(\text{COD})(1)_2^+, \text{BF}_4^-]$ (Phosphane protons; $[\text{CD-dim}] + [\text{Rh}] = 3 \text{ mM}$ in D_2O , 20°C).

VI) T-ROESY studies of the inclusion complexes

VI.1) T-ROESY of a Phosphane **1** and β -CD mixture

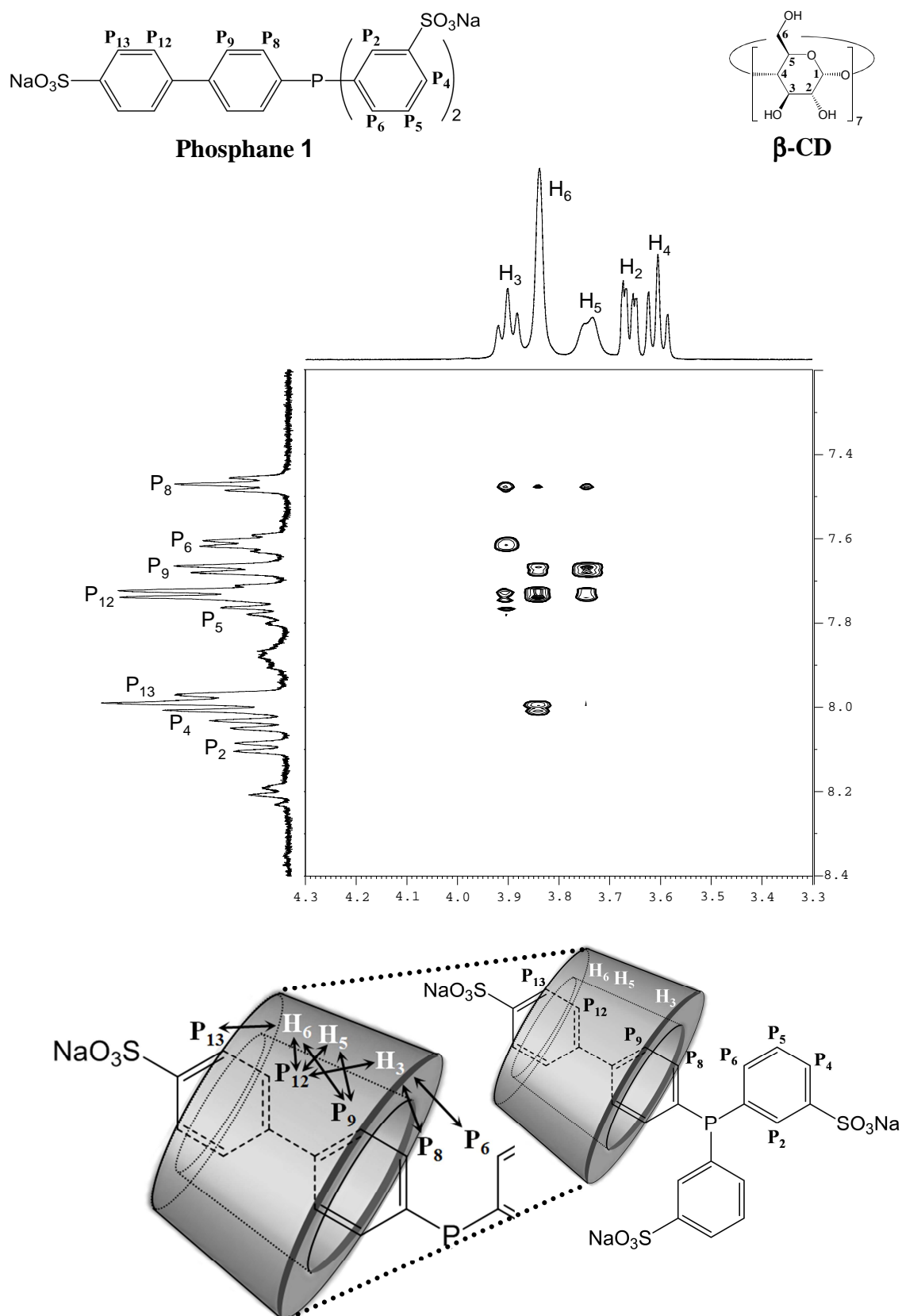


Figure S36: T-ROESY spectrum (500 MHz) of a **Phosphane 1** and β -CD mixture (3 mM / 7mM) in D₂O at 20°C.

VI.2) T-ROESY of a Phosphane 1 and CD-dim mixture

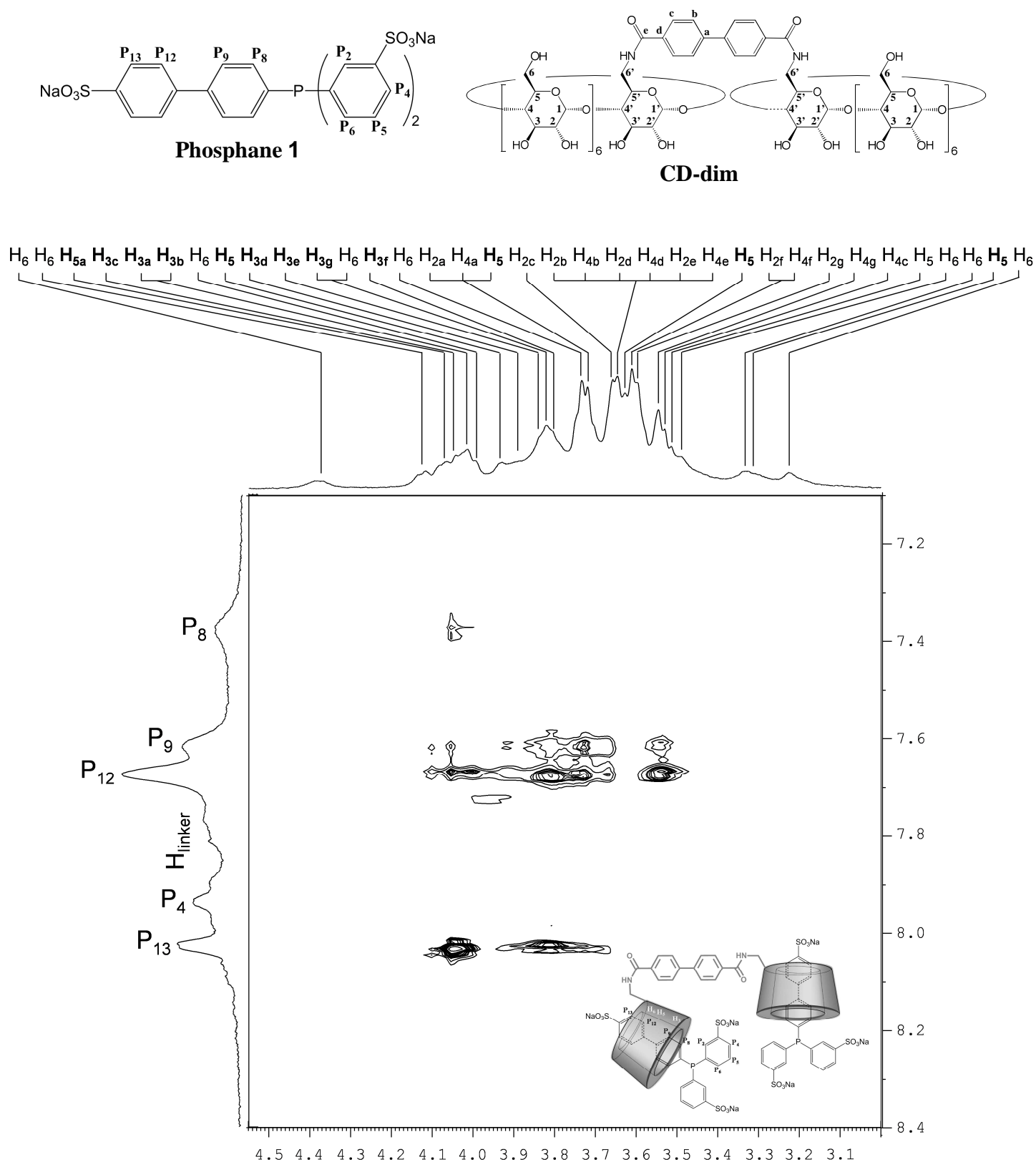


Figure S37: T-ROESY spectrum (600 MHz) of a **Phosphane 1** and **CD-dim** mixture (5 mM / 5mM) in D₂O at 20°C.

VI.3) T-ROESY of a $[\text{Rh}(\text{COD})(1)_2]^+$, BF_4^- complex and $\beta\text{-CD}$ mixture

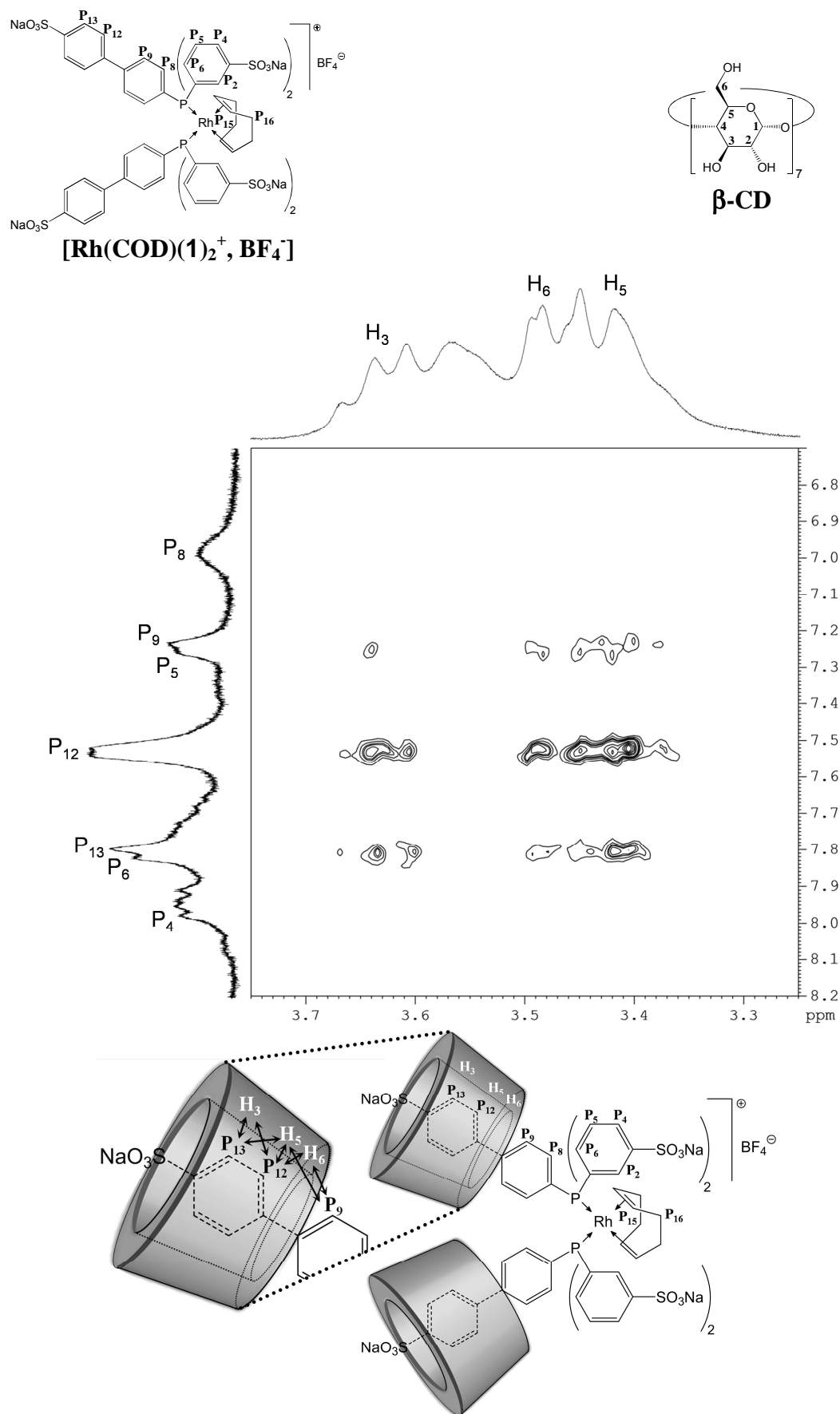


Figure S38: T-ROESY spectrum (300 MHz) of a $[\text{Rh}(\text{COD})(1)_2]^+$, BF_4^- and $\beta\text{-CD}$ mixture (3 mM / 6mM) in D_2O at 20°C .

VI.4) TROESY of a $[\text{Rh}(\text{COD})(1)_2^+, \text{BF}_4^-]$ complex and CD-dim mixture

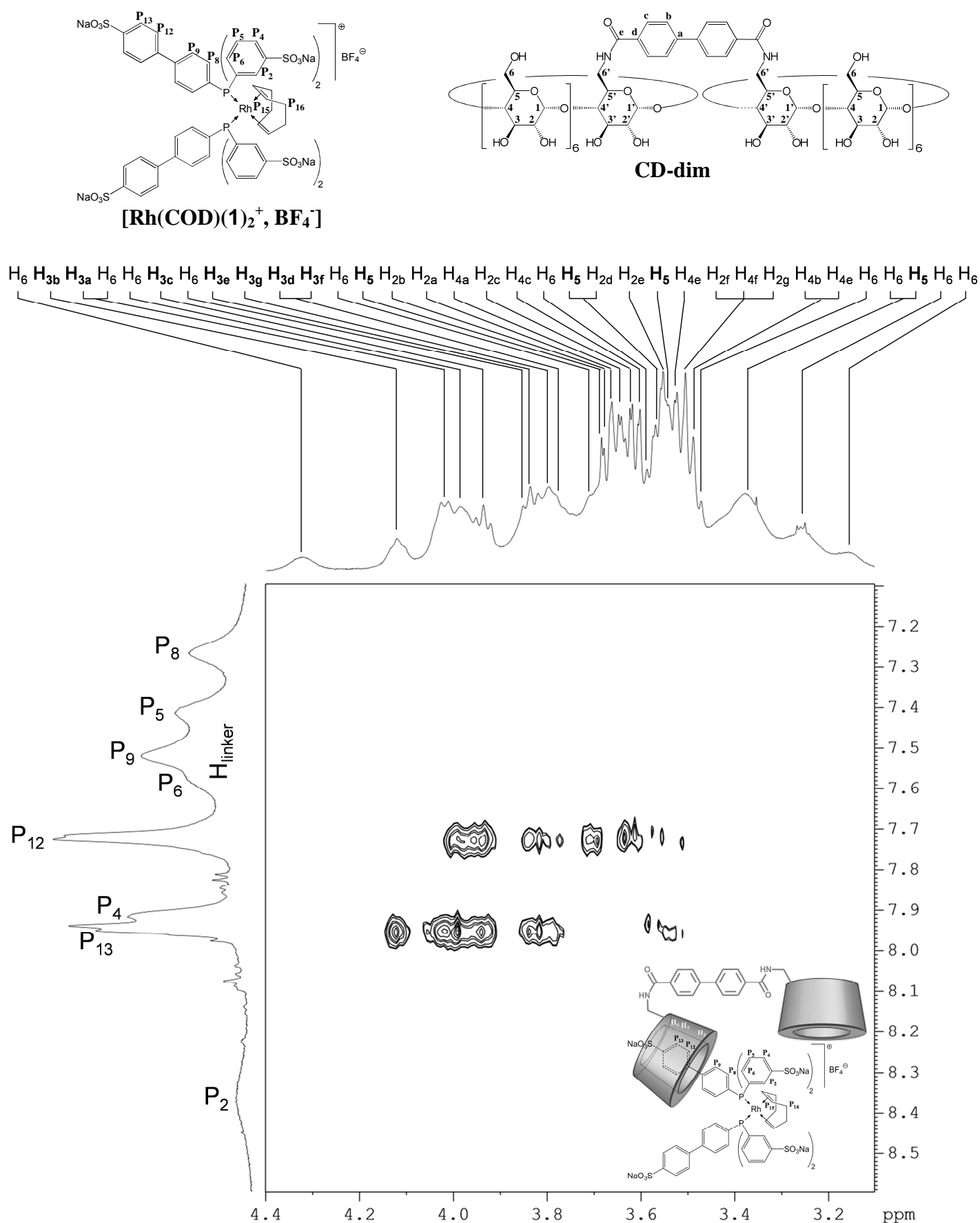


Figure S39: T-ROESY spectrum (600 MHz) of a $[\text{Rh}(\text{COD})(1)_2^+, \text{BF}_4^-]$ and CD-dim mixture (1.5 mM each) in D_2O at 20°C .

VII) Molecular dynamics simulations

♦ **Models** : Initial geometry for the **Rh(COD)(1)₂⁺** species was adapted from several structures taken in the Cambridge Structural Database (CSD)^[1] under the CULGOF^[2] and ALUZAI^[3] references. Geometry optimization was performed with the Gaussian09 program^[4] at the B3LYP level of theory using the 6-31+G* basis set for all atoms but Rhodium, which was described by the Stuttgart pseudopotential and associated basis set.^[5] In order to stay “bound”, a connected approach has been used to build the **Rh(COD)(1)₂⁺** species, where explicit covalent bonds have been set between the rhodium and its coordinating atoms. This step, requiring additional parameterization, was achieved using the FUERZA procedure^[6] and following a previous strategy used for ICL670 and iron.^[7]

Initial geometries of **CD-dim** were built using the LEaP program from the AmberTools 1.4 distribution, following the strategy and methodology previously established.^[8] Except for the linker, the CD fragments were taken from the R.E.DD.B. database^[9] under project F-85 (<http://q4md-forcefieldtools.org/REDDB/>). Both the linker fragment and the **Rh(COD)(1)₂⁺** were defined and parameterized according to the strategy developed previously using the RED program^[10] along with RED server.^[11] Computational conditions, charge values as well as force-field libraries required to build the complexes in this study were submitted to the R.E.DD.B. database and are freely available for download under the F-94 R.E.DD.B. project code.

♦ **Molecular Dynamics Simulations** : The SANDER module of the AMBER10 program suite was used to perform MD simulations on the aforementioned complexes.^[12] The systems were solvated in a truncated octahedral box with a buffer distance of 10.0 Å along with sodium counter-ions to neutralize the systems net charge. The q4md-CD force field parameters were used to model the β-CD systems.^[8] The parameters used for water were taken from the TIP3P model.^[13] After minimization, the systems were brought to target temperature by ramping up the temperature over periods of 25 ps followed by a run of 200 ps to relax and equilibrate the system. Classical MD simulations of 30 ns were then performed using the NPT ensemble at a pressure of 1 atm and a temperature of 300 K. The weak coupling algorithm^[14] was used to regulate the temperature and pressure. The temperature was maintained close to the intended value by weak coupling to an external temperature bath with a relaxation time of 2 ps and the pressure to an external pressure bath of 1 atm with a coupling constant of 2 ps. The SHAKE algorithm^[15] was used to constrain C-H bonds, and a time step of 2 fs was used to integrate the equations of motion. Periodic boundary conditions were imposed during simulation. The distance cutoff of 9.0 Å was applied to non-bonded interactions and the PME method^[16] was used to compute long-range interactions. Configurations of the systems were stored at intervals of 1 ps. Analyses of the trajectories were performed using the PTRAJ module available in the AmberTools 1.4. Visualization of the trajectories was achieved using the VMD package.^[17]

♦ Study of the possibility of a double inclusion of $\text{Rh}(\text{COD})(1)_2^+$ in CD-dim cavities (structure **B**) :

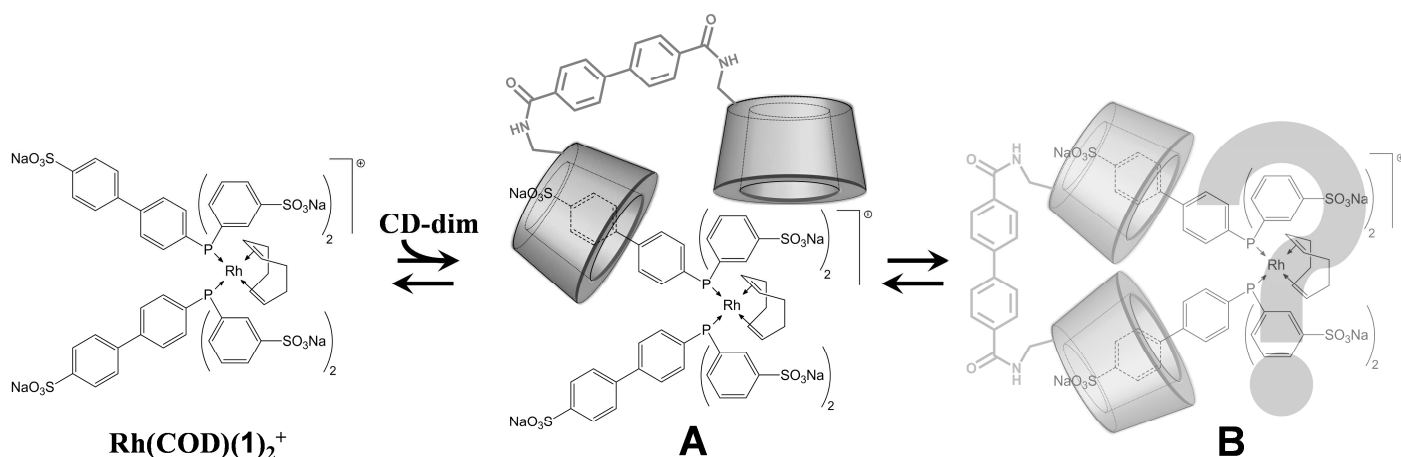


Figure S40: Systems **A** and **B** studied by molecular dynamics.

Molecular dynamics simulations of the **A** and **B** systems were performed in explicit water, with starting geometries imposed to be such as represented on Figure S40.

Figure 41 reports the distances between the center of mass of each CD cavity of **CD-dim** and the sulfur atom of the biphenyl group of each phosphane in the $[\text{Rh}(\text{COD})(1)_2^+, \text{BF}_4^-]$ species during the 30 ns of simulation.

The structure of the system **A** proved to be a very stable association throughout the 30 ns of simulations (Figure 41 a).

Conversly, the **B** structure did not stay in the double inclusion scheme (Figure 41 b). Many unsuccessful attempts to obtain an actual and stable **B** structure were made: either the complex **B** transformed into an **A** structure, or rhodium species and CD-dimer separated (Figure 41b) or the calculation stopped because of too important conformational clashes. The rigidity of the linker with the steric hindrance produced by the adjacent glucosidic units make the double inclusion phenomenon a very unlikely event.

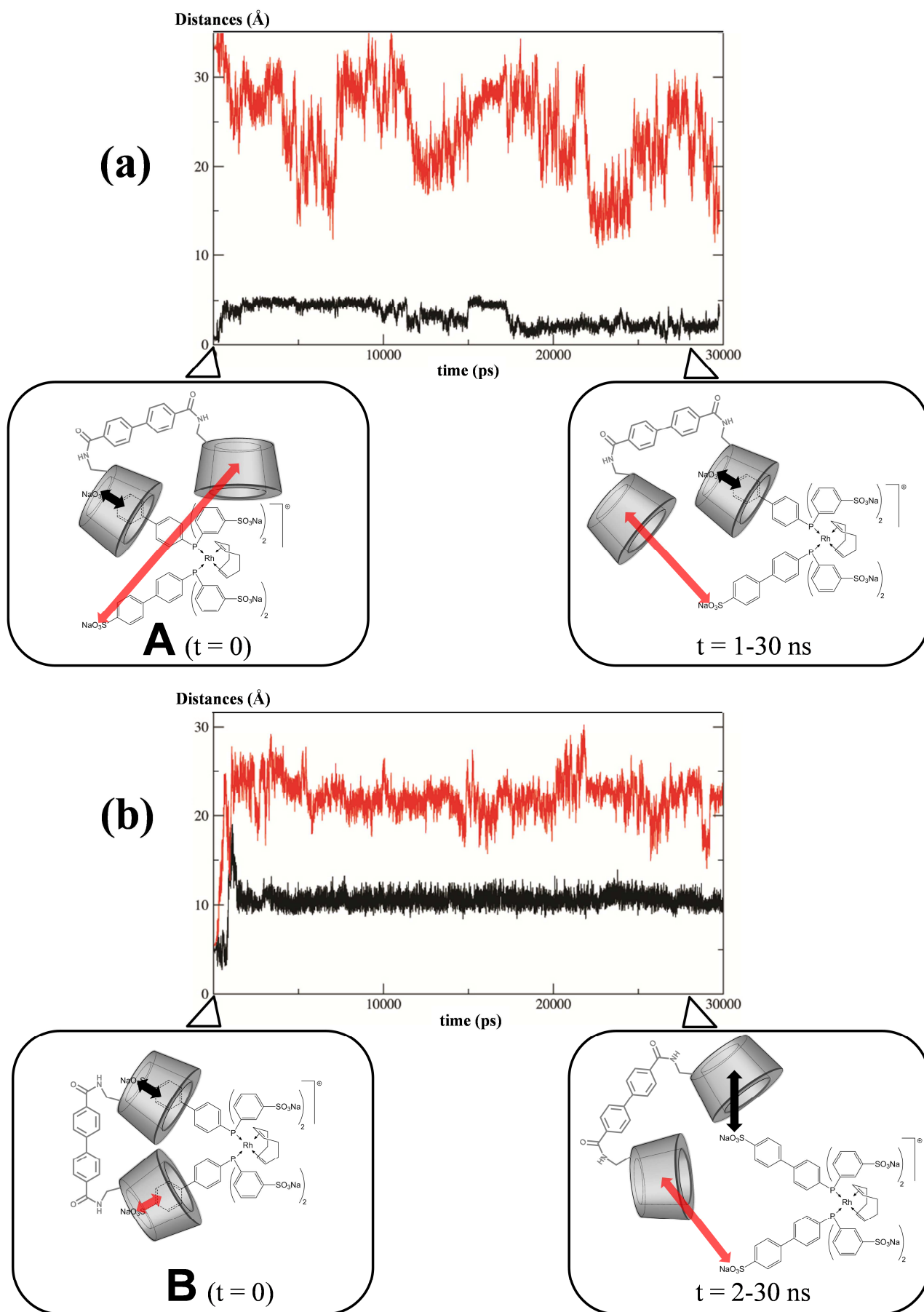
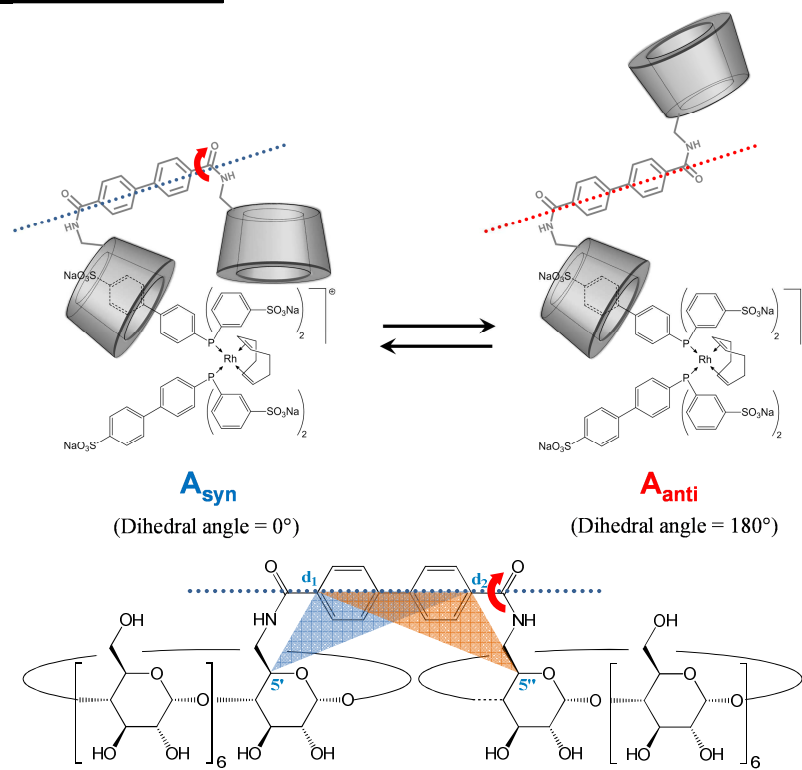


Figure S41. Evolution with time of the distances between the center of mass of each CD cavity of **CD-dim** and the sulfur atom of the biphenyl group of each phosphane of **Rh(COD)(1)₂⁺** for **(a) A** structure and **(b) B** structure (red and black curves correspond to the distances defined on the chemical formulas).

♦ Conformational study of **A** structure



Dihedral angle = angle between (C_{5'}, C_{d1}, C_{d2}) plan and (C_{d1}, C_{d2}, C_{5''}) plan

Figure S42. Equilibrium between **A_{syn}** and **A_{anti}** conformations and definition of the dihedral angle.

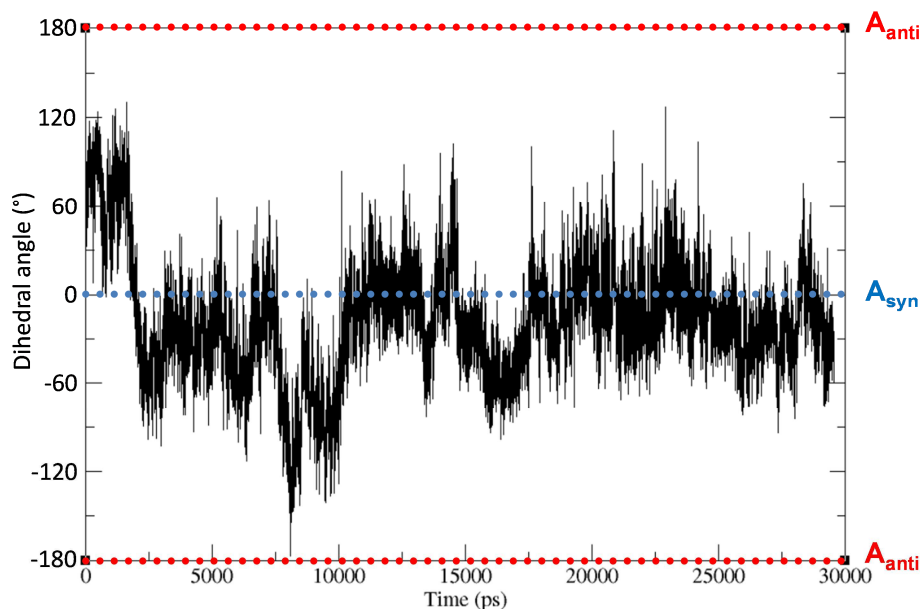


Figure S43. Evolution with time of the dihedral angle in **A** (dihedral angle=180° at t=0).

Statistically, the **A_{anti}** conformation for the two CD units does exist, but is a very infrequent event in the simulations performed. In all the simulations performed, the **A_{syn}** conformation was always preferred.

VIII) Tensiometry study of an aqueous solution of CD-dim

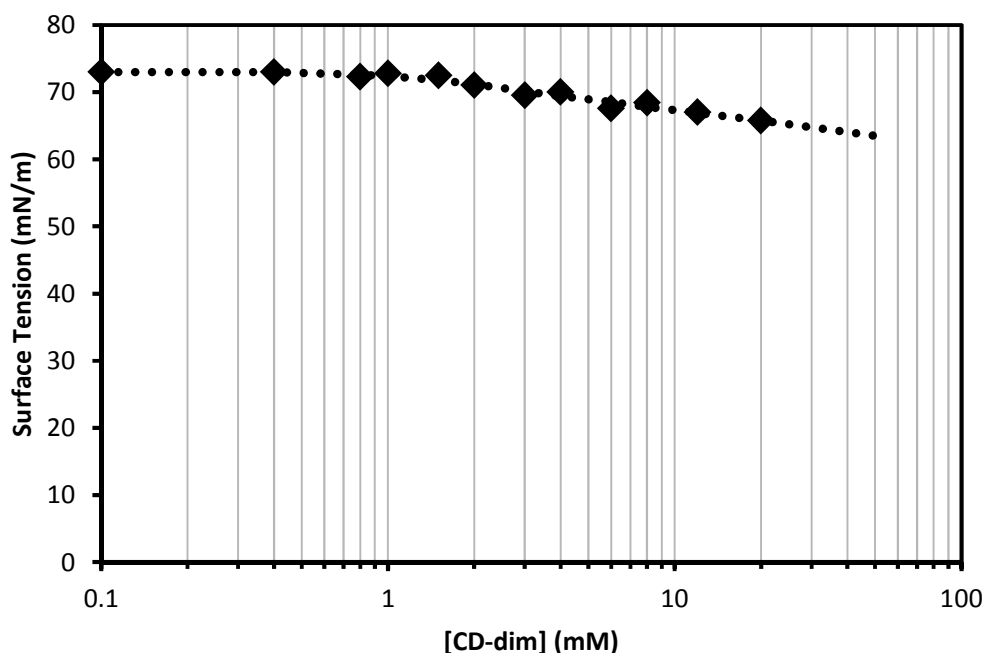


Figure S44. Evolution of surface tension of an aqueous solution of **CD-dim** vs concentration (20°C).

This curve was obtained with a Sigma 70 KSV automatic tensiometer. The Wilhelmy plate method was used. A concentrated solution of **CD-dim** was installed in the syringe of a dispenser connected to the tensiometer. Small volumes of this solution were added in a glass vessel containing ultrapure water at 20°C. After each addition, the solution is gently stirred for 1 minute and the surface tension was then determined after 5 minutes.

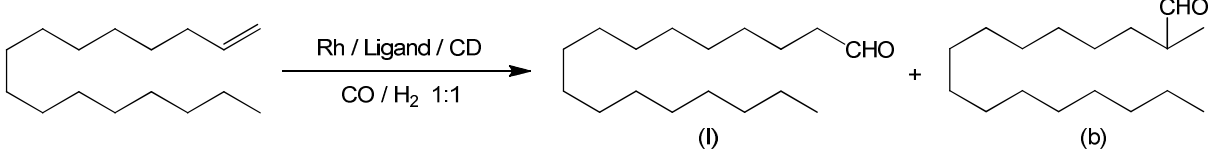
IX) Catalysis results

Table S2: Rhodium-catalyzed hydroformylation of 1-decene in the presence of various combinations [Ligand/CD derivative] ^[a]

Entry	Ligand	CD derivative	C (%) ^[b]	S (%) ^[c]	l/b
1	Phosphane 1	(-)	2	69	3.1
2	TPPTS	(-)	5	65	2.7
3	Phosphane 1	β-CD	40	77	2.2
4	TPPTS	β-CD	45	89	1.9
5	Phosphane 1	CD-dim	99	94	2.1
6	TPPTS	CD-dim	49	78	2.0

^[a] Conditions: Rh(acac)(CO)₂ = 21 μmol (5.5 mg), ligand = 105 μmol (5 eq.), CD cavity = 210 μmol (10 eq.), substrate = 10.5 mmol (500 eq.), 6 mL water, 80°C, 50 bar CO/H₂, 1500 rpm, reaction time = 9h. ^[b] C = 1-decene conversion. ^[c] S = aldehydes selectivity.

Table S3: Rhodium-catalyzed hydroformylation of 1-hexadecene in the presence of various combinations [Ligand/CD derivative] ^[a]

					
Entry	Ligand	CD derivative	C (%) ^[b]	S (%) ^[c]	I/b
1	Phosphane 1	(-)	3	47	2.6
2	TPPTS	(-)	3	56	2.6
3	Phosphane 1	β-CD	27	48	2.6
4	TPPTS	β-CD	24	50	2.7
5	Phosphane 1	CD-dim	53	54	2.6
6	TPPTS	CD-dim	20	57	2.9

^[a] Conditions: Rh(acac)(CO)₂ = 21 μmol (5.5 mg), ligand = 105 μmol (5 eq.), CD cavity = 210 μmol (10 eq.), substrate = 10.5 mmol (500 eq.), 6 mL water, 80°C, 50 bar CO/H₂, 1500 rpm, reaction time = 9h. ^[b] C = 1-hexadecene conversion. ^[c] S = aldehydes selectivity.

Table S4: Extra-conversions (%) observed with the [Phosphane 1 / CD-dim] system compared to the other [Phosphane 1 / β-CD], [TPPTS / β-CD] and [TPPTS / CD-dim] combinations and for 1-decene and 1-hexadecene as substrate

Entry	Ligands	CD derivative	E _{decene} ^[a]	E _{hexadecene} ^[a]
1	Phosphane 1	β-CD	+148%	+96%
2	TPPTS	β-CD	+120%	+120%
3	TPPTS	CD-dim	+102%	+165%

^[a] For a given substrate and a given [Ligand/CD derivative] reference combination, extra-conversion (E(%)) obtained with the [**Phosphane 1/CD-dim**] system was defined from the conversion obtained with the [**Phosphane 1/CD-dim**] system (C(%)) and the conversion obtained with the reference combination (C_{ref}(%)) by the following formula: E_{substrate} (%) = ((C - C_{ref})/C_{ref}) × 100.

The water-solubilities of 1-decene and 1-hexadecene at 80°C were equal to 10 μM and 0.2 μM, respectively. ^[18-20]

- [1] F. H. Allen, *Acta Crystallogr., Sect. B* **2002**, 58, 380-388.
- [2] M. Beller, H. Trauthwein, M. Eichberger, C. Breindl, J. Herwig, T. E. Müller, O. R. Thiel, *Chem. Eur. J.* **1999**, 5, 1306-1319.
- [3] C. Pettinari, F. Marchetti, R. Pettinari, A. Pizzabiocca, A. Drozdov, S. I. Troyanov, V. Vertlib, *J. Organomet. Chem.* **2003**, 688, 216-226.
- [4] M. J. Frisch, G. W. Trucks, H. B. Schlegel, G. E. Scuseria, M. A. Robb, J. R. Cheeseman, G. Scalmani, V. Barone, B. Mennucci, G. A. Petersson, H. Nakatsuji, M. Caricato, X. Li, H. P. Hratchian, A. F. Izmaylov, J. Bloino, G. Zheng, J. L. Sonnenberg, M. Hada, M. Ehara, K. Toyota, R. Fukuda, J. Hasegawa, M. Ishida, T. Nakajima, Y. Honda, O. Kitao, H. Nakai, T. Vreven, J. Montgomery, J. A. , J. E. Peralta, F. Ogliaro, M. Bearpark, J. J. Heyd, E. Brothers, K. N. Kudin, V. N. Staroverov, R. Kobayashi, J. Normand, K. Raghavachari, A. Rendell, J. C. Burant, S. S. Iyengar, J. Tomasi, M. Cossi, N. Rega, N. J. Millam, M. Klene, J. E. Knox, J. B. Cross, V. Bakken, C. Adamo, J. Jaramillo, R. Gomperts, R. E. Stratmann, O. Yazyev, A. J. Austin, R. Cammi, C. Pomelli, J. W. Ochterski, R. L. Martin, K. Morokuma, V. G. Zakrzewski, G. A. Voth, P. Salvador, J. J. Dannenberg, S. Dapprich, A. D. Daniels, Ö. Farkas, J. B. Foresman, J. V. Ortiz, J. Cioslowski, D. J. Fox, Gaussian, Inc., Wallingford CT, **2009**.
- [5] D. Andrae, U. Häußermann, M. Dolg, H. Stoll, H. Preuß, *Theoret. Chim. Acta* **1990**, 77, 123-141.
- [6] J. M. Seminario, *Int. J. Quantum Chem.* **1996**, 30, 1271-1277.

- [7] P. Rouge, A. Dassonville-Klimpt, C. Cézard, S. Boudesocque, R. Ourouda, C. Amant, F. Gaboriau, I. Forfar, J. Guillon, E. Guillon, E. Vanquelef, P. Cieplak, F.-Y. Dupradeau, L. Dupont, P. Sonnet, *ChemPlusChem* **2012**, *77*, 1001-1016.
- [8] C. Cezard, X. Trivelli, F. Aubry, F. Djedaini-Pilard, F. Y. Dupradeau, *Phys. Chem. Chem. Phys.* **2011**, *13*, 15103-15121.
- [9] F.-Y. Dupradeau, C. Cézard, R. Lelong, E. Stanislawiak, J. Pêcher, J. C. Delepine, P. Cieplak, *Nuc. Acids Res. - Database Issue* **2008**, D360-D367.
- [10] F.-Y. Dupradeau, A. Pigache, T. Zaffran, C. Savineau, R. Lelong, N. Grivel, D. Lelong, D. Rosanski, P. Cieplak, *Phys. Chem. Chem. Phys.* **2010**, *12*, 7821-7839.
- [11] E. Vanquelef, S. Simon, G. Marquant, E. Garcia, G. Klimerak, J. C. Delepine, P. Cieplak, F. Y. Dupradeau, *Nucleic Acids Res.* **2011**, *39*, W511-W517.
- [12] D. A. Case, T. A. Darden, I. Cheatham, T. E, C. L. Simmerling, J. Wang, R. E. Duke, R. Luo, M. Crowley, R. C. Walker, W. Zhang, K. M. Merz, B. Wang, S. Hayik, A. Roitberg, G. Seabra, I. Kolossvary, K. F. Wong, F. Paesani, J. Vanicek, X. Wu, S. R. Brozell, T. Steinbrecher, H. Gohlke, L. Yang, C. Tan, J. Mongan, V. Hornak, G. Cui, D. H. Mathews, M. G. Seetin, C. Sagui, V. Babin, P. A. Kollman, **2008**.
- [13] W. L. Jorgensen, J. Chandrasekhar, J. D. Madura, R. W. Impey, M. L. Klein, *J. Chem. Phys.* **1983**, *79*, 926-935.
- [14] H. J. C. Berendsen, J. P. M. Postma, W. F. van Gunsteren, A. Dinola, J. R. Haak, *J. Chem. Phys.* **1984**, *81*, 3684-3690.
- [15] J. P. Ryckaert, G. Ciccotti, H. J. C. Berendsen, *J. Comput. Phys.* **1977**, *23*, 327-341.
- [16] U. Essmann, L. Perera, M. L. Berkowitz, T. A. Darden, H. Lee, L. G. Pedersen, *J. Chem. Phys.* **1995**, *103*, 8577-8593.
- [17] W. Humphrey, A. Dalke, K. Schulten, *J. Molec. Graphics* **1996**, *14*, 33-38, 27-38.
- [18] K. Wakita, M. Yoshimoto, S. Miyamoto and H. Watanabe, *Chem. Pharm. Bull.*, **1986**, *34*, 4663-4681.
- [19] B. S. N. Murty, Y. Kumar, N. V. K. Dutt and P. J. Reddy, *Phys. Chem. Liq.*, **1997**, *34*, 77-87.
- [20] P. Ruelle and U. W. Kesselring, *Chemosphere*, **1997**, *34*, 275-298.